The Persistent Radical Effect: A Principle for Selective Radical Reactions and Living Radical Polymerizations

Hanns Fischer*

Physikalisch-Chemisches Institut, Universität Zürich, Winterthurerstrasse 190, CH-8057 Zürich, Switzerland

Received March 23, 2001

Contents

I. Introduction

From time to time reactions involving both transient and persistent radical intermediates were discovered that lead to a highly dominant and unusually selective formation of the cross-reaction products of these radicals. The usual transient radical self-terminations are virtually absent, although chain processes are not involved. This remarkable phenomenon was seldom explained, although it has a quite simple basis.

Consider the mechanism of Scheme 1, where transient R• and persistent radicals Y• are formed simultaneously with equal rates from the same or different precursors (1, 2). Then, from the usual radical−radical reactions (3, 4) one obtains R−Y as highly dominant product.

Scheme 1

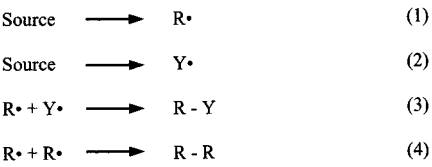

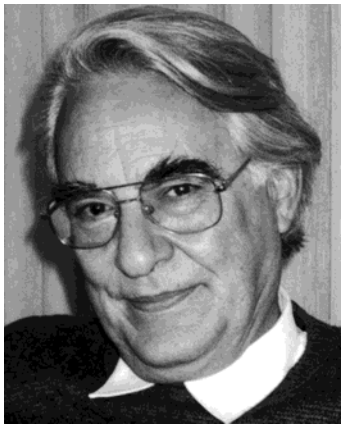

Hanns Fischer, born 1935, started his carreer at the Technical University Darmstadt, Germany, and obtained his Ph. D. (1963) and Habilitation (1966) working at the Deutsches Kunststoff-Institut mostly on polymer-related transient carbon-centered free radicals with ESR, NMR and CIDNP. After leading a physicochemically oriented division of this Institute, a period at Carnegie-Mellon University, Pittsburgh, and lecturing in Darmstadt, he became Associate (1969) and then full Professor (1971) for Physical Chemistry at the University of Zürich, Switzerland. There, he continued his work on transient organic free radicals, their structure, reaction mechanisms, and reaction kinetics in liquid solutions employing ESR, CIDNP, optical spectroscopy, and muon spin rotation. He has authored about 240 original publications, several reviews, and two books and edits a large series of tables on radical properties and kinetics in Landolt-Börnstein. Honors include the Centenary Medal and Lectureship of the Chemical Society London and the Silver Medal of the International EPR Society. He retires in 2001 but intends further research on the topic of this review.

* To whom correspondence should be addressed. Phone: +41 1 635 4421. Fax: +41 1 635 6856. E-mail: hfischer@pci.unizh.ch.

10.1021/cr990124y CCC: $36.00
Published on Web 11/07/2001

Offhand, one may be surprised. Intuitively, one could expect equal concentrations of R• and Y•, because the radicals are formed with equal rates, and therefore, the products R−Y and R−R should be formed in the statistical ratio of 2:1. However, this is not the case, except during a very short initial period. The simple cause is that the transient radicals R• disappear by their self-termination (4) and by the cross-reaction, whereas by definition the persistent radicals Y• do not self-terminate but disappear only by the cross-reaction.[1] Hence, every self-termination event of R• (3) causes a buildup of excess Y•, and this buildup continues as the time goes on. The permanently increasing concentration of Y• accelerates the cross-reaction at the expense of the self-termination (4). This reaction never stops completely but attains lower and lower levels. Hence, R−Y becomes the main product. In fact, a dynamic equilibrium is reached where the rate of the cross-reaction matches that of the radical generation (1, 2). This leads to the following general conclusions:

(1) If the transient and persistent radicals are formed with equal rates, one always expects the highly dominant formation of their cross-reaction products, be it R−Y formed by the combination (3), products such as R(−H) and Y−H arising from a disproportionation, or ions such as R^+ and Y^- resulting from a charge-transfer between R• and Y•.

(2) If the transient radicals R• transform rapidly into other transient radicals R′•, for example by fragmentation, rearrangement, addition to an unsaturated molecule, atom or group transfer, or by any other reaction, then the cross-reaction products between R′• and Y• become dominant. The transformation of Y• to another persistent Y′• leads to the selective formation of R−Y′.

(3) During the reactions, the concentration of the persistent species Y• increases to a much higher level than the concentrations of the transient radicals R• or R′•.

Yet, these statements leave open questions. How persistent must Y• be to cause this effect, and are equal formation rates really necessary? We answer them later and first consider Scheme 2.

Scheme 2

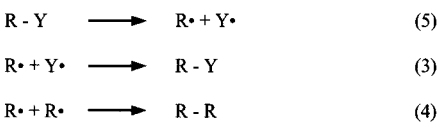

The two radicals are now produced by the reversible dissociation of a common precursor R−Y but undergo the same reactions as in Scheme 1, otherwise. Now, the above argumentation suggests:

(4) The lifetime of the radical precursor R−Y is markedly prolonged because it is permanently regenerated, and the dynamic equilibrium between the radical generation and the cross-reaction acts like the chemical equilibrium of the reversible decay.

(5) A rapid transformation of R• into R′• leads again mainly to R′−Y, if the formation of this product is irreversible, and a transformation of Y• to another persistent Y′• leads again to R−Y′.

However, one may reason now that one will not find a marked lifetime prolongation if the equilibrium constant is above a critical limit. Actually, a too small rate constant of the back-reaction must lead to a fast and complete conversion of R−Y to the final products R−R and Y•. Also, the self-termination of the transient radicals never ceases completely. Therefore, a true stationary state does not exist, and for the given reaction mechanism, the radical concentrations will always depend on time. Moreover, the apparent equilibrium and the lifetime prolongation of R−Y are only of transient nature, because at sufficiently long times one must always find only self-termination products and persistent radicals.

A technically important situation arises when the transformation of R• to R′• occurs by addition to a suitable monomer, M; the resulting product R′−Y = R−M−Y itself undergoes the fragmentation (5), R−M• undergoes further monomer addition, and the process continues. This mechanism is displayed in Scheme 3, where $n \geq 0$ denotes the number of monomer units that are contained in the radical and product species.

Scheme 3

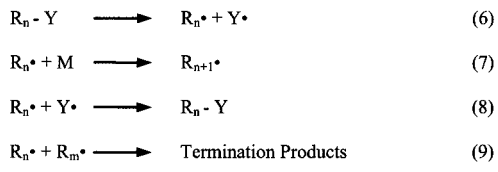

Carbon-centered radicals derived from the low molecular compounds R−Y and from the longer chain molecules R_n−Y have similar structures and reactivities, and therefore,

(6) one expects a polymerization without termination,[2] which is characterized by a transient equilibrium between the dormant polymer R_n−Y and the radicals.

(7) The dormant polymer is living in the sense that it grows until the monomer is depleted, and that it can grow on after additional monomer feed as in an ionic living polymerization.[3] The final degree of polymerization is determined by the initial concentrations of the monomer and of the radical precursor R_0−Y, and the formation of block copolymers is possible.

(8) One further obtains a controlled growth of the polymer if the characteristic time for the reversible dissociation is sufficiently short in comparison with monomer conversion, that is, if all chains start to grow practically together.[2]

However, one may again suspect that this will hold only under favorable kinetic circumstances.

So far, we have introduced the concept of what is now called the "persistent radical effect" without giving specific examples or theoretical proof for its existence. Further, we have indicated that there may be stringent conditions for its occurrence in real chemistry. This review further elucidates the phenomenon, but it is restricted to the most important aspects and to illustrative chemical systems. The next section shows how the main ideas have been developed over the years in order to explain specific

observations, and it reveals the fundamental kinetic conditions for basic reaction schemes. Then, we list a larger variety of examples from organic,[4] metal−organic, and polymer chemistry and close with an outline of an appropriate theoretical analysis and its application to further cases of practical interest.

Today, the subject is far from being mature. There are probably many more experimental manifestations of the effect than we are aware of, and there may be more kinetic peculiarities and variants. This is the reason we neither present a completely comprehensive description of all pertinent experimental findings nor a complete theory. Moreover, the particular subfield of living radical polymerizations involving the effect has become of practical importance. Hence, in the past few years, a large number of publications and patents have been published on this topic. These are covered in more detail in other parts of this issue, and here, we discuss only those aspects that are important for the operation of the persistent radical effect in living polymerizations.

II. Early References and Basic Kinetics

A. Non-Polymeric Systems

1. Leading Observations

To our knowledge, Bachmann et al.[5] were the first who stated the correct reason for the unusual preference for unsymmetrical coupling reactions in systems involving persistent and transient radicals as early as 1936. They had prepared phenyl- and *p*-biphenyl carrying pentaarylethanes and studied their stability. In oxygenated *o*-dichlorobenzene solutions containing pyrogallol as hydrogen donor, all compounds decomposed quantitatively at 100 °C within a few minutes to triarylmethyl and diarylmethyl hydroperoxides. Various experiments ensured that the primary dissociations to triarylmethyl and diarylmethyl radicals were followed by very fast additions of these radicals to oxygen and by the consecutive very fast hydrogen abstractions of the resulting peroxyradicals from pyrogallol (Scheme 4). Hence, the rates of conversion were equal to the rates of dissociation of the pentaarylethanes.

Surprisingly at first, the pentaarylethanes were much more stable under oxygen-free conditions.

Scheme 4

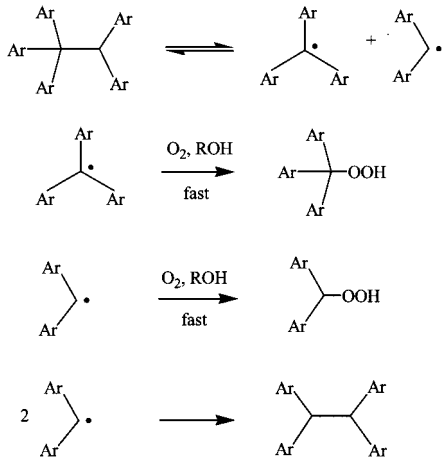

Thus, "penta-*p*-biphenylethane gave only two percent of *s*-tetra-*p*-biphenylethane after being heated for two hours in *o*-dichlorobenzene at 100 °C, the original compound being recovered in 87% yield." However, the solutions developed the characteristic color of triarylmethyl radicals, and this agreed with the much faster conversion under oxygen. The authors concluded that in the absence of oxygen, "the dissociation of pentaarylethanes is a reversible reaction in which the position of the equilibrium is practically entirely in favor of the pentaarylethane". They also knew that diarylmethyl radicals but not triarylmethyl radicals dimerize irreversibly under their experimental conditions and, hence, that in these systems diarylmethyl radicals are transient and triarylmethyl radicals are persistent species. Obviously, the cross-coupling between these is strongly favored.

To explain these observations the authors wrote "Now, the irreversible formation of an extremely small amount of *s*-tetraethylethane (by coupling, Scheme 4) results in a corresponding increase in the equilibrium concentration of triarylmethyl radicals; as a result the concentration of diarylmethyl radicals is reduced to such an extent that their association is practically stopped." Moreover, "The formation of every molecule of *s*-tetraarylethane decreases the rate of formation of the next molecule." They also clearly noticed the unusual character of the apparent dissociation equilibrium because "the concentration of triarylmethyl radicals is always much greater than the concentration of diarylmethyl radicals," and "this precluded measurements of the extent of the equilibrium from the color", that is, the triarylmethyl concentration. Finally, they noted that "it should be borne in mind, however, that a pentaarylethane solution is an unstable system which in infinite time would disproportionate completely into hexaarylethane ("triarylmethyl radicals" would be more appropriate) and *s*-tetraarylethane." These are the features of a persistent radical effect following Scheme 2.

The second thoughtful description was given by Perkins.[6] He explained the unusual product distributions of phenylations of aromatic compounds when phenylazotriphenylmethane is used as thermal phenyl radical generator. Scheme 5 provides an example. It had been found[7] that benzene solutions yield 1,4-dihydro-4-triphenylmethylbiphenyls as major products besides biphenyl and triphenylmethane, and "a particular feature of this scheme is the absence of dimerization and disproportionation of the interme-

Scheme 5

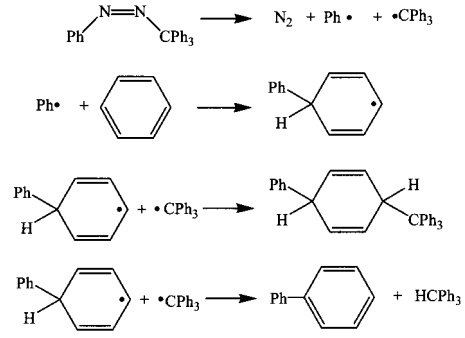

diate phenylcyclohexydienyl radical as both of these processes are known to occur in other systems."

Perkins cited more so far unexplained examples for the observation of simple product mixtures in reactions where triphenylmethyl radicals from phenylazotriphenylmethane were involved[8] and Bachmann's work.[5] Realizing the kinetics expected for Scheme 1, he wrote "The exceptional stability of triphenylmethyl radicals is probably responsible.... This is because any trace occurrence of radical-destroying processes which do not involve triphenylmethyl radicals must give rise to a high concentration of this stable species. The relatively high concentration of triphenylmethyl radicals can subsequently scavenge other radicals which are formed (with the exception of the very short-lived phenyl radical). Under stationary state-conditions triphenylmethyl radicals are being formed at the same rate as that at which they are being converted into products. Hence, the relatively high concentration is maintained, and the scavenging effect continues throughout the reaction." Thus, Perkins perceived the dynamic equilibrium as expected for Scheme 1. He also considered a variety of other manifestations for what he called "stable radical effects".[9]

Not being aware of the earlier work, the present author first noticed the phenomenon in 1981. Geiger and Huber[10] had photolyzed dimethylnitrosamine in the gas phase at 1 Torr and under 100 Torr N_2 buffer. This compound fragments from the first excited singlet state into dimethylaminyl radicals and nitrous oxide NO with unity quantum yield, but neither photoproducts nor a decrease of the initial compound pressure were observed. Even after 20 h photolysis the back-reaction was complete to more than 99.9% (Scheme 6). This seemed quite puzzling because sterically unhindered aminyl radicals are transient and readily self-terminate by coupling and disproportionation.

Scheme 6

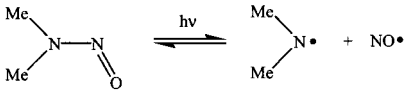

A few years later the author noticed a report by Kraeutler that stated that methylcobalamine is stable under photolysis in aqueous solution in the absence of radical scavengers, but that the presence of CO in moderate concentration (0.03 M) leads to acetylcobalamine in high yield.[11] The explanation (Scheme 7) was again unusual in view of the known propensity of methyl and acetyl radicals for rapid coupling reactions.

A discussion of these results led in 1985 to another independent formulation of the correct interpretation by Ingold. Nitrous oxide and the demethylated cobalamine are persistent and will increase in concentration because the transient radicals self-terminate, and the excess persistent species will then scavenge the transient ones.

2. Theoretical Description

Although the qualitative explanations by Bachmann,[5] Perkins,[6] and Ingold are very reasonable, it

Scheme 7

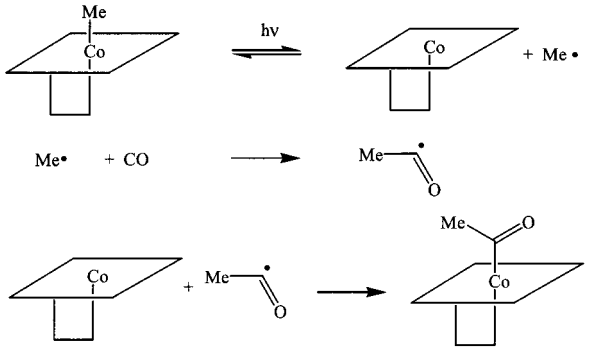

seemed worthwhile to investigate whether the extreme selectivity as, for example, reported by Huber et al.[10] can be rationalized quantitatively. To be more general, the reactions of Scheme 8 were used in our first theoretical analysis. It allowed for unequal rates of generation of the persistent and the transient radicals and for the self-terminations of both radicals.[12] We outline the major results here because they reveal the inner working of the mechanism but now use a simpler formalism.

Scheme 8

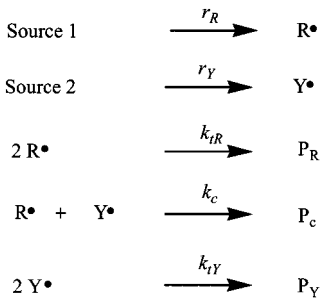

The radical concentrations are abbreviated as [R] and [Y], and the notations of Scheme 8 are used for the rates of radical generation (r) and for the rate constants (k) of the bimolecular radical reactions.[13] The radical concentrations obey the rate equations

$$d[R]/dt = r_R - k_c[R][Y] - k_{tR}[R]^2 \qquad (10)$$

and

$$d[Y]/dt = r_Y - k_c[R][Y] - k_{tY}[Y]^2 \qquad (11)$$

For the initial conditions $[R]_0 = [Y]_0 = 0$, both radical concentrations increase at first linearly in time, $[R] = r_R t$, $[Y] = r_Y t$, but at later times the behavior diverges. If all rate parameters are different from zero, a stationary state is found[12] where $d[R]/dt = d[Y]/dt = 0$. From this relation, the conditions on r_R and r_Y emerge for which the selectivity for the formation of the cross-reaction product P_c is a maximum. This selectivity may be defined by the ratio of the rate of the cross-reaction to the sum of the rates of product formation by the self-terminations, that is, by

$$s = \frac{k_c[R][Y]}{k_{tR}[R]^2/2 + k_{tY}[Y]^2/2} = \frac{2(k_c/k_{tR})[Y]/[R]}{1 + (k_{tY}/k_{tR})([Y]/[R])^2} \quad (12)$$

Differentiation with respect to the auxiliary variable [Y]/[R] yields the maximum of s for $[Y]/[R] = (k_{tR}/k_{tY})^{1/2}$. Use of this relation and eqs 10 and 11 for the stationary state and subtraction of the resulting equations 13 and 14 yields $r_R = r_Y$:

$$d[R]/dt = 0 = r_R - k_c(k_{tR}/k_{tY})^{1/2}[R]^2 - k_{tR}[R]^2 \quad (13)$$

and

$$d[Y]/dt = 0 = r_Y - k_c(k_{tR}/k_{tY})^{1/2}[R]^2 - k_{tR}[R]^2 \quad (14)$$

Hence, the maximum selectivity does occur in fact for equal formation rates of the two radicals, as was implied in the discussions of Schemes 1 to 3 and as is valid for the mechanisms of Schemes 4−7. Restricting the further discussion to the case $r_R = r_Y = r$ at the moment and using $[Y]/[R] = (k_{tR}/k_{tY})^{1/2}$ and eq 12 provide

$$s_{max} = \frac{k_c}{(k_{tR}k_{tY})^{1/2}} \quad (15)$$

Now, if Y• were as transient as R•, one would have approximately $k_{tR} = k_c = k_{tY}$, which gives $s_{max} = 1$. This leads to the statistical product distribution $[P_R]:[P_C]:[P_Y] = 1:2:1$. However, for a persistent Y• with a small self-termination constant $k_{tY} \ll k_c \approx k_{tR}$ one obtains $s_{max} \gg 1$.[14] For instance, if the rate constant for the self-termination of Y• were $k_{tY} = 10^3$ M^{-1} s^{-1} and the other rate constants diffusion controlled, $k_c = k_{tR} \approx 10^9$ M^{-1} s^{-1} in nonviscous liquids, the selectivity would become $s_{max} \approx 1000$, and this means 99.9% cross-reaction. Hence, the selectivity increases with decreasing self-termination rate constant of the persistent species; however, this species need not be infinitely long-lived. Further, one notes that $[Y]/[R] = (k_{tR}/k_{tY})^{1/2}$ implies $[Y] \gg [R]$ for $k_{tR} \gg k_{tY}$, that is, the large excess of the persistent radical. Moreover, for $k_{tY} \ll k_c \approx k_{tR}$ the self-termination terms on the right-hand sides of eqs 13 and 14 are much smaller than the cross-reaction term. This proves the existence of a dynamic equilibrium

$$k_c[R][Y] = r \quad (16)$$

for which the rate of radical generation is nearly completely balanced by the rate of the cross-reaction.

Our treatment explained the experimental results of Huber et al.[10] and Kraeutler[11] quantitatively.[12] However, it is not strictly applicable when Y• does not self-terminate at all because [Y]/[R] and s diverge to infinity for $k_{tY} \to 0$. Actually, in this case and for equal rates of radical generation, eqs 10 and 11 have no stationary state solution except for infinite time, where [Y] goes to infinity and [R] becomes zero.

Figure 1 shows computed time evolutions of the radical concentrations for $[Y]_0 = [R]_0 = 0$, a common radical generation rate $r = 10^{-6}$ M s^{-1}, $k_{tR} = k_c = 10^9$ M^{-1} s^{-1}, and different ratios k_{tY}/k_{tR} in a log−log representation.[12] Such log−log representations are unusual, but they are needed here and in the following because they allow one to clearly visualize the different time regimes. The interpretation of the time evolution is straightforward. For all ratios of the self-termination constants, both radical concentrations first increase linearly with time, $[R] = [Y] = rt$. When the rate of the terminations become approximately equal to the rate of radical generation, [R] attains a maximum, in times of milliseconds to seconds for usual rate constants. Thereafter, the concentration of the transient radical decreases, and the excess of the persistent species builds up. For nonzero self-termination of the persistent radical, both radical concentrations reach stationary states. For $k_{tY} = 0$, however, [R] continues to decrease and [Y] continues to increase. After the maximum of [R], log [R] and log [Y] depend linearly on time. They show slopes of different signs but equal magnitude. For $k_{tY} = 0$, this holds forever, and it is observed also for a nonzero k_{tY} before the stationary states are reached. The magnitudes are smaller than 1, that is, in this regime the time dependencies of both radical concentrations are weak. Empirically, the slopes give $[Y] \sim t^{1/3}$ and $[R] \sim t^{-1/3}$, and such time dependencies are very unusual in chemical kinetics. Furthermore, one finds empirically that the concentrations obey the dynamic equilibrium eq 16.

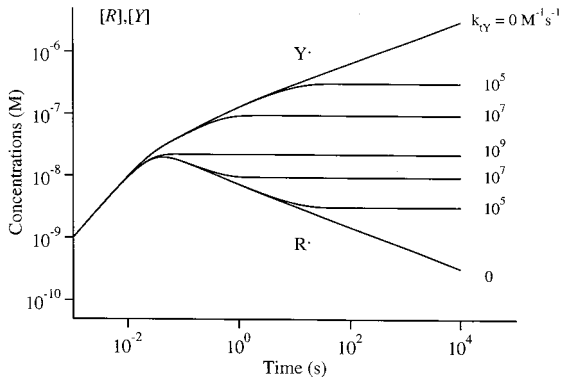

Figure 1. Computed time dependencies of the concentration of the transient (R•) and the persistent radicals (Y•) for $[Y]_0 = [R]_0 = 0$, a common radical generation rate $r = 10^{-6}$ M s^{-1}, $k_{tR} = k_c = 10^9$ M^{-1} s^{-1}, and different ratios k_{tY}/k_{tR} in a log−log representation. The log−log representation enhances the visualization of the different time regimes.

A rigorous derivation of the unusual time dependencies and of eq 16 for $k_{tY} = 0$ was first found for the reversible radical generation of Scheme 2 with the restriction $k_{tR} = k_c$,[15] which was removed subsequently.[16,17] The mathematical method will be outlined in section IV. For the mechanism of Scheme 8, with equal radical formation rates and $k_{tY} = 0$, it provides for the radical concentrations at sufficiently long times[18]

$$[R] = (r/3k_ck_{tR})^{1/3}\, t^{-1/3} \quad \text{and}$$
$$[Y] = (3k_{tR}r^2/k_c^2)^{1/3}t^{1/3} \quad (17)$$

They fulfill the dynamic equilibrium relation (16).

For the reversible radical generation of Scheme 2 and $k_{tY} = 0$, the unusual time dependencies $[Y] \sim t^{1/3}$ and $[R] \sim t^{-1/3}$ and the large excess of [Y] over [R]

are also valid. In eqs 17, r must be replaced by $k_d[I]_0$ where k_d is the rate constant of the dissociation of the radical precursor R−Y, and $[I]_0$ is its initial concentration so that[15−17]

$$[R] = (K[I]_0/3k_{tR})^{1/3}\, t^{-1/3} \quad \text{and}$$
$$[Y] = (3K^2 k_{tR}[I]_0{}^2)^{1/3} t^{1/3} \quad (18)$$

where $K = k_d/k_c$. Equation 16 now reads

$$k_c[R][Y] = k_d[I]_0 \quad (19)$$

This is the equilibrium relation for the reversible dissociation with the actual time-dependent concentration of the precursor replaced by its initial value.[19] However, the stoichiometry of the reactions of Scheme 2 requires that the concentration of the persistent radical cannot exceed the initial precursor concentration. This limits the kinetic parameters for which eqs 18 and 19 are valid to

$$K \ll k_c[I]_0/k_{tR}, \quad K \ll [I]_0, \quad \text{and} \quad k_d \le k_{tR}[I]_0 \quad (20)$$

The first of these conditions is the strongest. They also provide an upper time limit for the operation of the persistent radical effect,[17] but such an upper limit does not exist for the case of continuous radical generation.

As anticipated in the Introduction, for a system following Scheme 2, the equilibrium constant of the precursor dissociation must not be larger than an upper limiting value. If this holds, one obtains a lifetime of the precursor R−Y that exceeds the natural lifetime $(k_d)^{-1}$ by the factor of $k_c[I]_0/k_{tR}K$, and this may amount to many orders of magnitude.[15−17]

An insertion of realistic rate parameters shows that the second and the third of the conditions (11) are not critical. For instance, the rate constant k_d for the dissociation of R−Y will normally not exceed $k_d = 1$ s^{-1}, because the compound will otherwise be very unstable, even at low temperatures. Experimental rate constants for the reaction of transient with persistent radicals are normally larger than 10^6 M^{-1} s^{-1}. Hence, a realistic upper limit of the equilibrium constant is $K = 10^{-6}$ M. Self-termination constants of transient radicals are normally diffusion-controlled, that is, $10^{10} > k_{tR} > 10^8$ M^{-1} s^{-1}, and finally, practical aspects set the lower limit of the precursor concentration to $[I]_0 = 10^{-3}$ M. Hence, the second and the third of the conditions (11) read $K < 10^{-6}$ M $\ll [I]_0$ and $k_d/k_{tR} < 10^{-8}$ M $\ll [I]_0$ and are always well obeyed. For these numbers, one has $k_c[I]_0/k_{tR} = 10^{-7}$ M. Obviously, the first condition is not met for the extreme parameters chosen here, but it will be fulfilled for a lower equilibrium constant, a larger initiator concentration, and a larger cross-coupling constant.

3. Experimental Verifications

The early theoretical conclusions on chemical systems following Scheme 8[12] prompted a first experimental verification.[20] Transient *tert*-butyl radicals were generated by photolysis of di-*tert*-butyl ketone in *n*-heptane. Simultaneously and in the same solu-

Scheme 9

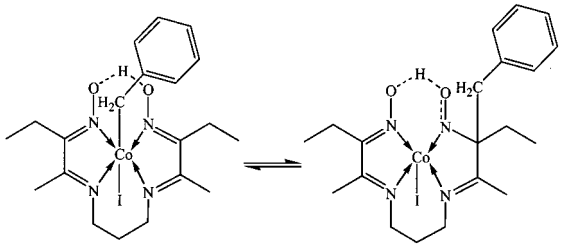

Scheme 10

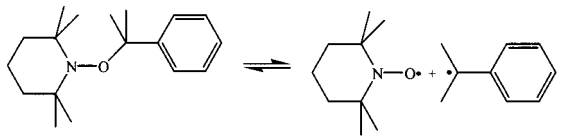

tions, the persistent 2,4,6-tri-*tert*-butylphenoxyl radical ($k_{tY} \approx 0$) was generated by hydrogen abstraction from the phenol by photolytically produced *tert*-butoxy radicals, and the rate of generation of *tert*-butyl was varied by changing the ketone concentration. ESR spectra taken during continuous reaction revealed a dramatic decrease of the *tert*-butyl concentration to unobservably low levels when its rate of formation became equal to or lower than that of the persistent species. This is well-described by the appropriate analytic equations. Moreover, time-resolving experiments on the two-radical system showed that the transient radical concentration decayed completely to zero when the radical generation was interrupted. On the other hand, a marked residue of 2,4,6-tri-*tert*-butylphenoxyl radicals was leftover even when the transient species was produced in excess, and we will comment on the kinetics in section IV. Use of the semipersistent 2,6-di-*tert*-butyl-4-methylphenoxyl radical ($k_{tY} \approx 10^{-8}$ M^{-1} s^{-1} at room temperature) showed less dramatic effects of the relative rate of radical generation but also supported the theoretical expectations.

A second, and more chemical, verification is due to Finke et al.,[21] who also invented the descriptive phrase "persistent radical effect" and gave a prototype example to the extreme. The thermal reversible 1,3-benzyl migration in a coenzyme B_{12} model complex leads to the equilibrium of Scheme 9. Earlier work had shown that the reaction involves freely diffusing benzyl and persistent cobalt macrocycle radicals, but the expected self-termination product bibenzyl of benzyl was missing. Extending the detection limits, the authors found traces of bibenzyl and deduced a selectivity for the formation of the cross-products to the self-termination products of 100 000: 1 or 99.999%. Kinetic modeling further showed that over a time of 1000 years only 0.18% of bibenzyl would be formed, and this stresses the long-time duration of the phenomenon.

More recently, the unusual time-dependence of the radical concentrations (9) was also observed directly.[22] Like many other *N*-alkoxyamines (trialkylhydroxylamines), 2-phenyl-2-(2′,2′,6′,6′-tetramethylpiperidine-1′-oxyl)propane (cumyl-TEMPO) (Scheme 10) cleaves thermally reversibly into a persistent nitroxide radical (TEMPO) and a transient carbon-

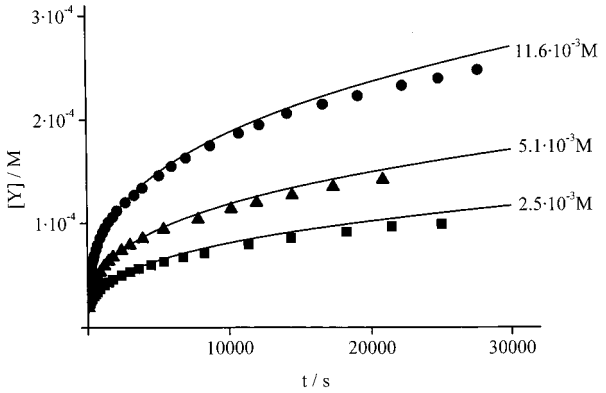

Figure 2. Time dependence of the TEMPO concentration during thermolysis of cumyl-TEMPO in *tert*-butylbenzene for different initial cumyl-TEMPO concentrations at 83 °C. The solid lines confirm the $t^{1/3}$-dependence (eq 18).

centered radical (cumyl). The time evolution of the nitroxide concentration is easily followed by ESR spectroscopy, and the result is shown in Figure 2. The solid lines correspond to the expected $t^{1/3}$-dependence (eq 18) with the parameter combination $(3k_{tR}K^2[I]_0^2)^{1/3}$ evaluated at the beginning of the curves. Slight deviations at long times are due to a concurring disproportionation between TEMPO and cumyl, which leads to the hydroxylamine and α-methylstyrene in about a 1% yield.

Variations of the initial alkoxyamine concentration $[I]_0$ and independently measured rate constants k_d, k_c, and k_{tR} nicely confirmed that the system fulfills the conditions (20) and reproduced the value of the parameter combination taken from the experimental data. The same was found for other alkoxyamines.[16,23] However, it must be mentioned that the observation of such kinetics requires precautions with respect to the purity of chemicals, solvents, and containers. This is necessary because even very minor side reactions may strongly interfere with the many cycles of dissociation and recoupling that are necessary to provide a clear kinetic manifestation of the effect.

B. Polymer Systems

1. Leading Observations

The development of living and controlled radical polymerizations has been stimulated considerably by early work of Otsu dating back about 20 years ago.[24] His concepts center around the reversible reaction of a suitably end-capped polymer chain providing a chain radical that can add to monomer and a persistent species. In 1982 he noted "in order to find a system of living radical polymerization in homogeneous solution, one must try to form propagating polymer chain ends which may dissociate into a polymer with a radical chain end and small radicals which must be stable enough not to initiate a new polymer chain." He also presented the formal Scheme 11 and mentioned the possibility of a stepwise growth that would lead to molecular weight control.

Otsu knew of the tendency of stable radicals to undergo primary radical cross-termination and was aware of some of the earlier work on triphenylmethyl

Scheme 11

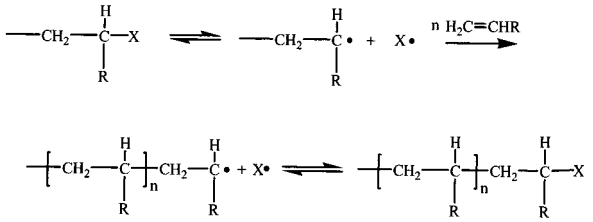

and related persistent radicals. However, he did not mention the excess of the persistent over the transient species or give a reason for the propensity of the cross-reaction. At first, he employed phenylazotriphenylmethane as initiator to polymerize methyl methacrylate at 60 °C. Indeed, the molecular weight increased linearly with the conversion, as is expected for a controlled process.[2] Livingness was demonstrated by the observation "when the polymer was heated at 80 °C in the presence of the monomer, polymerization was induced and the molecular weight of the polymer increased markedly" and "These findings strongly suggest that the monomer molecules were inserted into the carbon−triphenylmethyl bond, as the result of a radical dissociation." Otsu also found that in the absence of monomer the polymer was stable in benzene at 80 °C, although there must be dissociation, and this is a clear sign for the lifetime prolongation. In further work, Otsu[24] and Braun et al.[25] used initiators dissociating into two semipersistent radicals that both can initiate and also tend to cross-terminate. Features of living and controlled polymerizations were again achieved, but the conversions and the molecular weights of the resulting polymers were rather low.

Two further elements of Otsu's early work are also noteworthy, because they are related to more recent (and more successful) developments: First, he used the reversible halogen atom exchange between low valent metal compounds, in particular Ni(0), and organic halides as initiating and regulating system.[26] The polymers obtained from heterogeneous mixtures were partly living and controlled, and this work anticipates the mechanism now called "atom transfer radical polymerization". Second, he showed[24] that the polymerization of methyl methacrylate with phenylazotriphenylmethane is unusually slow but that it is markedly accelerated by the addition of a conventional initiator without loss of polymer livingness.

In 1985, Rizzardo et al.[27] filed a patent for the use of alkoxyamines (Scheme 12) as regulating initiators for the living radical polymerization and block copolymerization of vinyl monomers. R is a group that upon dissociation (Scheme 10) forms a radical that adds to the monomer. The mechanism was disclosed shortly thereafter and involves the reversible dissociations shown in Scheme 11, with the nitroxide radical taking the role of X.[28] In a later simulation, the group also revealed the reason for the remarkable absence of the usual terminations and rediscovered the principles of the persistent radical effect:[29] "As chains undergo termination transient radicals are removed from the system and the concentration of persistent species builds". Further, the authors noted correctly that, in contrast to normal radical polymer-

Scheme 12

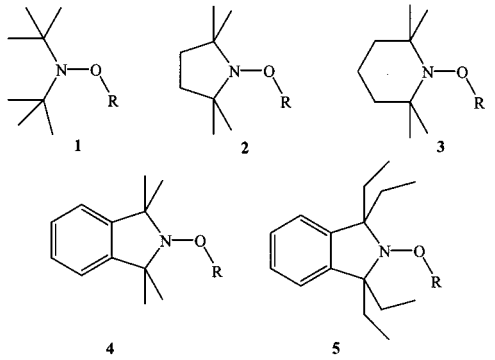

Scheme 13

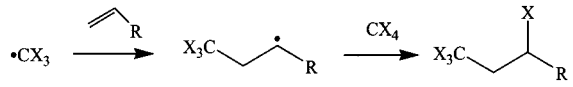

Scheme 14

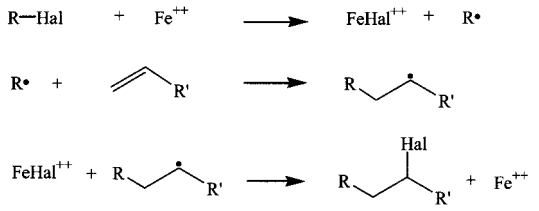

izations with essentially constant radical concentrations, no steady-state approximation is possible.

Whereas the patent stressed the controlled formation of oligomers and low molecular weight polymers, Georges et al. showed in 1993 that moderate molecular weight (50 000 au) polystyrenes with low polydispersity indices (1.20) can be obtained by nitroxide-mediated polymerizations at around 120 °C.[30] Instead of using alkoxyamines as initiators, they employed a 1.2:1 ratio of the nitroxide radical TEMPO (Scheme 10, and **3** in Scheme 12) and dibenzoyl peroxide in styrene and preheated the reaction mixture to 95 °C for a short time. Under these conditions, benzoyloxy radicals first add to styrene. The coupling of the adduct radicals with TEMPO provides unimeric alkoxyamines that initiate the polymerization at the higher temperature. As expected for a stepwise growth, the degree of polymerization increases fairly linearly with conversion. It was also noticed that a larger initial excess of the persistent species decreased the polydispersity at the expense of a slower polymerization rate. Later work showed, among other results, that the concentration of the persistent nitroxide increases during the polymerization, because of the ongoing termination, that the rate of polymerization can be increased considerably by a slow removal of the excess nitroxide, that these controlled polymerizations display no gel effect, and that they can be extended to aqueous-phase polymerizations and also to the formation of polystyrene−polybutadiene, −polyisoprene and −polyacrylate block copolymers.[31]

The technical potential of the work of Rizzardo et al.[27−29] and Georges et al.[30,31] stimulated further research along similar lines by many other groups. We mention here only a few principally important and early results. By an elegant crossover experiment using model polystyrene alkoxyamine derivatives, Hawker et al.[32] demonstrated the occurrence of the reversible cleavage. The prolongation of the alkoxyamine lifetime during the reactions became evident from the apparent decay times reported for 1-phenyl-1-(2′,2′,6′,6′-tetramethylpiperidine-1′-oxyl)ethane (phenethyl-TEMPO) by Priddy et al.[33a] of about 150 min in trichlorobenzene at 140 °C and by Hawker et al.[33b] of about 5 min in styrene at 123 °C. In the latter case, the addition of the 1-phenethyl radical to styrene prevents the regeneration of the parent compound, of course. Further, it was often noticed that the polymerization rates obtained in many nitroxide-mediated processes are unconveniently small, even at temperatures as high as 130 °C, and this is so because the persistent radical effect leads to very low transient radical concentrations.

Using di-*tert*-butylnitroxide (DBNO)-based initiators (**1** in Scheme 12), Catala et al.[34] observed that the polymerization rate of styrene is independent of the initiator alkoxyamine concentration. This is unusual in radical polymerizations, and Matyjaszewski et al.[35a] first pointed out in this case that the styrene polymerization rate is governed by the autoinitiation of the monomer that creates additional propagating species. These authors also published illuminating simulations on the nitroxide-mediated process.[35b] The autoinitiation of styrene then may have led to the renewed idea[36] to add a slowly decomposing conventional initiator to the systems. This had already been realized by Otsu.[24] Sparingly applied, it accelerates the polymerizations appreciably without deteriorating the livingness and the control to untolerable extents.[36]

The facile and reversible dissociation of cobalt−carbon bonds to give a persistent cobalt-derived and a transient alkyl radical was discussed already in connection with Schemes 7 and 9. In 1994, it was first utilized by Wayland et al.[37] in living and controlled polymerizations of methyl acrylate. Using (tetramesitylporphyronato)cobalt neopentyl and variants thereof in benzene solution at 60 °C provided only oligomers for small ratios of monomer to complex, but for ratios of 2500:1, polymers with M_n = 150 000 and about 70% conversion were achieved. The molecular weight increased linearly with conversion, and the polydispersity index was as low as 1.1−1.3. Livingness of the polymer, that is, the fidelity of the porphyrinatocobalt end group of the polymer chains, was demonstrated by the formation of block copolymers of methyl and butyl acrylate. Wayland knew of the earlier publications on the persistent radical effect[12,21] and interpreted his findings in terms of Scheme 3.

The addition of polyhaloalkanes and related halogenated compounds to alkenes can occur via a classical radical chain process (Scheme 13), which is often called the Kharasch reaction.[38] In 1961, Minisci et al.[39] and Asscher and Vofsi[40] discovered that this reaction is catalyzed by transition metal ions in their lower valent state such as Cu^+ and Fe^{2+}, and they formulated the mechanism in Scheme 14. The catalysis of the additions by simple metal salts or complexes such as Cu(I)-2,2′-bipyridyl[41a] and ruthe-

nium(II) tris(triphenylphosphine) ($RuCl_2(PPh_3)_3$)[41b] found many organic synthetic applications. It was often stated that the intermediacy of freely diffusing carbon-centered radicals is unlikely in these processes, because the normal termination products are absent. However, the transition metal ions and their complexes are persistent, and Scheme 14 involves the simultaneous formation of a persistent species and a transient radical. Hence, the operation of the persistent radical effect is a much more likely cause for the virtual absence of the self-termination reactions.

Monoadditions are usually carried out with about 1:1 ratios of the organic halide and the alkene and very small catalyst concentrations. When lower halide/alkene ratios are used, telomer formation is important. Hence, for small halide concentrations, high polymers may be obtained, and this is supported by Otsu's experiments[26] with Ni(0) powders.

The first real success along these lines was achieved in 1995 by Sawamoto et al.,[42] Matyjaszewski et al.,[43] and Percec et al.[44] The first group used $RuCl_2(PPh_3)_3$ as catalyst and CCl_4 as initiating halide in a 1:2 ratio, added methylaluminum bis(2,6-di-*tert*-butylphenoxide) to activate the initiator C−Cl bonds, and employed methyl methacrylate as monomer solvent. Nearly 90% conversion was achieved at 60 °C in about 4 h.[42] Matyjaszewski employed Cu(I)Cl-2,2′-dipyridyl (1:3) as catalyst and 1-chloro-1-phenylethane (1) as initiator and found 90% conversion of styrene in about 3 h at 130 °C.[43] The polymerization of styrene was also addressed by Percec et al.,[44] who used the same catalyst as Matyjaszewski but diverse aromatic sulfonyl chlorides as initiators. All authors amply demonstrated the livingness of the resulting polymers and the controlled nature of the process with molecular weights increasing with conversion and low polydispersities. In comparison to Otsu's earlier attempt,[26] their success is presumably due to the more homogeneous reaction conditions following from the use of metal complexes. Since the addition of haloalkanes to alkenes involves atom transfer steps, Matyjaszewski termed the new method "atom transfer radical polymerization" (ATRP).[43] In terms of polymerization rates and generality, ATRP appears to be the most versatile variant of living radical polymerizations based on the persistent radical effect today.

2. Theoretical Description

Before entering the kinetic treatment of living radical polymerizations based on the persistent radical effect, it is necessary to define the terms "living" and "controlled" radical polymerization as used in this review, because a unified terminology has not yet evolved and conflicting views have been expressed.[45] In the sense of Szwarc,[3] we call a polymer "living" that, after formation and isolation, can grow upon further monomer feed and that can be used to build block copolymers. The dormant chains formed in nitroxide and cobalt-complex-mediated polymerizations carry end groups that provide transient radicals upon dissociation to which monomer can add. Hence, these processes are properly "living". In ATRP, the dormant chains carry halogen atoms as end groups. Alone and freed from the catalyst they will not initiate new polymerizations, but they revive upon addition of the same or another catalyst. Therefore, in a looser sense we will consider these processes also as "living" polymerizations. By "controlled" we mean a polymerization for which the number-average degree of polymerization (X_N) and, hence, the number-average molecular weight of the polymer increase linearly with monomer conversion and for which X_N ideally reaches the ratio of the initial monomer and initiator concentrations at full monomer conversion. These are the characteristics of a polymerization without termination.[2] If, in addition, all chains start in a time period that is short compared to the overall conversion time, that is, practically at the same time, one obtains a narrow Poisson chain length distribution. Then, the polydispersity index develops as $PDI = M_W/M_N = X_W/X_N = 1 + 1/X_N$ and decreases with increasing conversion to values close to one.[2]

"Livingness" and "control" go parallel in many ionic processes, but this need not always be so. Actually, in the radical polymerizations, the dissociation of the dormant chains or the activating halogen transfer may be so slow that considerable conversion occurs before these reactions have occurred at least once. Then, one expects the formation of a polymer with a large "living" fraction but little "control". On the other hand, if the time for appreciable monomer conversion overlaps with the final reaction stage where the termination processes dominate, one may find products with a large degree of "control" but little "livingness".

The theoretical exploration of living radical polymerizations has been approached by numerical simulations of conversion rates and molecular weight distributions. Several methods have been developed.[15,17,29,35,46,47] Such simulations provide considerable insight into the inner working of the mechanisms and can reproduce the experimental findings. Yet, they are not of general value, because they hold only for the specific kinetic parameters employed in the individual cases. For the analysis of polymerization data, analytical equations are more helpful, and their derivations also reveal the fundamental kinetic aspects. Such derivations address the time dependence of the radical concentrations, of the monomer conversions, and of the evolution of the molecular weight distributions, and they have mainly been worked out by Fukuda et al. and by our group.

Before giving some results, it must be stressed that all equations have been derived and will be valid only for ideal cases, especially only for chain length independent rate constants and in the absence of any reactions besides those considered explicitly. Further, they imply mathematical approximations. Both restrictions can lead to deviations of the experimental data from the theoretical results. Yet, such deviations do not disprove the equations, unless it is demonstrated that the preconditions of the derivations are strictly fulfilled by the chemical systems under study.

In our work,[15−17] we have mainly concentrated on polymerizations that follow Schemes 3 and 11. Dis-

proportionation was assumed as a general mechanism for the irreversible termination. The latter restriction is not serious, because termination by coupling would simply double the molecular weight of the dead polymer fraction, which should anyway be small.

Since the rate constants, including those of the primary radicals, shall not depend on chain length, the total radical concentrations obey eqs 18, and the equilibrium relation (19) is established if the conditions (20) are fulfilled. The only additional equation is the rate equation for the conversion of the monomer M

$$\frac{d[M]}{dt} = -k_p[R][M] \tag{21}$$

and it does not change the evolution of the concentrations of R$^\bullet$ and Y$^\bullet$. It is easy to show that there will be very little conversion before the equilibrium regime is established.[17] To obtain the conversion in this regime, one inserts eq 18 for [R] into eq 21 and integrates to

$$[M] = [M]_0 e^{-3/2k_p\left(\frac{K[I]_0}{3k_t}\right)^{1/3} t^{2/3}} \quad \text{or}$$

$$\ln\frac{[M]_0}{[M]} = \frac{3}{2}k_p\left(\frac{K[I]_0}{3k_t}\right)^{1/3} t^{2/3} \tag{22}$$

(The index R of k_{tR} is dropped here and in the following because k_{tY} is always assumed to be zero).

For a conventional polymerization with a constant rate of initiation r_I and constant radical concentration $[R]_s = (r_I/k_t)^{1/2}$, one has the relation[2]

$$[M] = [M]_0 e^{-k_p[R]_s t} \quad \text{or} \quad \ln\frac{[M]_0}{[M]} = k_p[R]_s t \tag{23}$$

The difference between eqs 22 and 23 is due to the time dependence of [R] in eq 18.

Polymerization in the equilibrium regime does provide the control of the molecular weight and a narrow molecular weight distribution. The integration of the kinetic equations for the moments of the distribution (see section IV) leads to equations for the number-average degree of polymerization (X_N) and the polydispersity index PDI = $M_W/M_N = X_W/X_N$.

$$X_N = \frac{[M]_0 - [M]}{[I]_0(1 - e^{-k_d t})} \tag{24}$$

$$PDI = 1 - e^{-k_d t} + \frac{1}{X_N} + \frac{[M]_0^{\,2}}{([M]_0 - [M])^2}(1 - e^{-k_d t}) \times \left(\frac{\pi k_p{}^3[I]_0}{k_d k_c k_t}\right)^{1/2} \operatorname{erf}\left[(3k_p)^{1/2}\left(\frac{K[I]_0}{3k_t}\right)^{1/6} t^{1/3}\right] \tag{25}$$

If the dissociation of the initiator occurs well before the conversion ($k_d t \gg 1$), all chains start to grow practically together at zero time. Then eq 24 provides the desired linear increase of M_N with the conversion and the control by the initial initiator concentration. The PDI decreases with increasing X_N, time, and conversion, and the last term in eq 25 with the error function (erf) reflects the residual influence of the terminations. At short times one has

$$PDI_0 = 1 + \frac{1}{X_N} + \frac{8}{3k_d t} \tag{26}$$

and at infinite time the PDI becomes

$$PDI_\infty = 1 + \frac{[I]_0}{[M]_0} + \left(\frac{\pi k_p{}^3[I]_0}{k_d k_c k_t}\right)^{1/2} \tag{27}$$

For properly chosen rate parameters it attains values close to one. Figures 3 and 4 display the behavior of the polymerization index (X_N) and PDI as computed and as predicted by eqs 22, 24, and 25.

The livingness of the polymer is also easily calculated because the number of dead chains is practically equal to the number of the released persistent species, which is known from eq 18. Further, the analytical solutions provide conditions for the rate constants that should allow a successful living and controlled polymerization.[17] First, we may want the concentration fraction of the dead polymer products $[P]/[I]_0$ at the large monomer conversion of 90% to

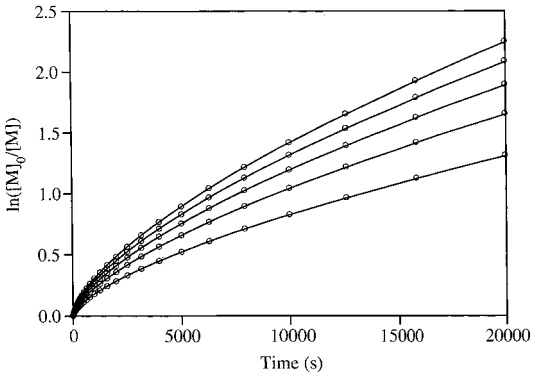

Figure 3. Polymerization index $\ln([M]_0/[M])$ vs time during a polymerization in the equilibrium regime for k_p = 5000 M^{-1} s^{-1}, $k_t = 10^8$ M^{-1} s^{-1}, k_d = 0.0045 s^{-1}, $k_c = 2.2\cdot10^7$ M^{-1} s^{-1}, $[M]_0$ = 10 M, and $[I]_0$ = 0.02, 0.04, 0.06, 0.08, and 0.1 M as obtained by numerical integrations and eq 22 (circles).

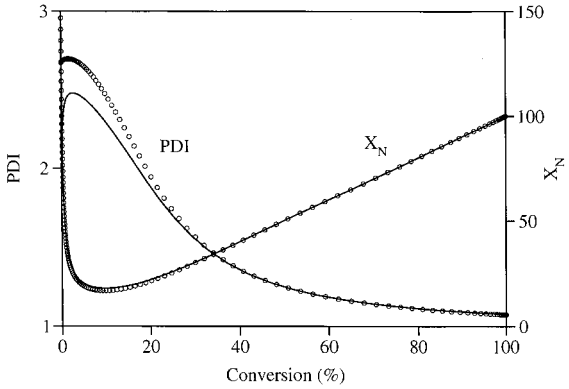

Figure 4. Evolution of the total number-average degree of polymerization X_N and the polydispersity index with conversion during a polymerization in the equilibrium regime for k_p = 5000 M^{-1} s^{-1}, $k_t = 10^8$ M^{-1} s^{-1}, k_d = 0.0045 s^{-1}, $k_c = 2.2\cdot10^7$ M^{-1} s^{-1}, $[M]_0$ = 10 M, and $[I]_0$ = 0.1 M as obtained by numerical integrations and eqs 24 and 25 (circles).

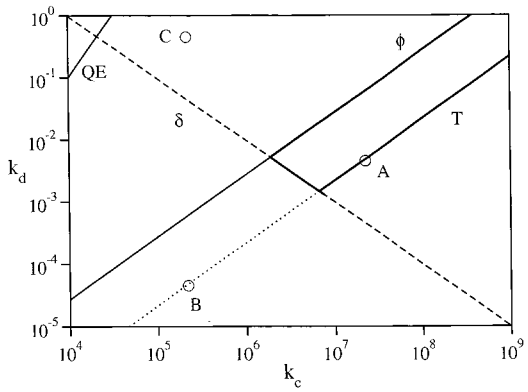

Figure 5. Graphical representation of the kinetic conditions for the existence of the quasiequilibrium (QE, eq 20), a small fraction $\phi < 5\%$ of unreactive polymer, a small residual polydispersity $\delta < 0.2$, and a time $T < 20\,000$ s (5.55 h) for 90% conversion. $k_t = 10^8$ M^{-1} s^{-1}, $k_p = 5000$ M^{-1} s^{-1}, and $[I]_0 = 0.1$ M. The region where all conditions are obeyed is emphasized by a heavy frame. It should be noticed that the diagram holds only for the absence of initial persistent species and radical generation only from the regulator $I_0 = R_0 - Y$.

be below an allowed upper limit ϕ. From eqs 18 and 22 this requires

$$K = \frac{k_d}{k_c} \leq \frac{k_p[I]_0}{2\ln(10)k_t}\phi^2 \tag{28}$$

Second, the residual polydispersity index PDI $= 1 + 1/X_N$ should be smaller than an upper limiting value δ, and hence, from eq 26

$$k_d k_c \geq \frac{\pi k_p{}^3[I]_0}{k_t}\frac{1}{\delta^2} \tag{29}$$

Third, the time needed for 90% conversion should not exceed a time T, which is dictated by technical limitations such as working hours. Equation 22 shows this to be the case if

$$K = \frac{k_d}{k_c} \geq \frac{(2\ln(10))^3 k_t}{9k_p{}^3[I]_0 T^2} \tag{30}$$

Obviously, large equilibrium constants yield short conversion times at the expense of larger dead polymer fractions. This need not conflict with the desired control, however, since the molecular weight and the polydispersity index do not directly depend on K but on k_d (24) and on the product $k_d k_c$ (27).

The optimum values of k_d and k_c depend on the propagation constant (k_p), the termination constant (k_t), and the attempted degree of polymerization through $[I]_0$. For a given set of these latter parameters one finds a range for k_d and k_c in which a living and controlled polymerization should be observed. This is illustrated by the diagram shown in Figure 5, which was constructed with the aid of eqs 28−30. Here, point A corresponds to the rate constants leading to Figure 4, that is, to a process yielding 90% conversion in 5.55 h for a monomer with $k_p = 5000$ M^{-1} s^{-1}, an average degree of polymerization $X_N = 100$, a polydispersity index of 1.2, and 5% dead chains. Along a line from point A to point B, K is constant, but k_d and the product $k_d k_c$ decrease. Hence, one obtains in the same time as for case A a polymer with the same small dead fraction, but it shows much less control. On the other hand, along the line from point A to point C, K and k_d increase but the product $k_d k_c$ stays constant. Now, one expects a polymer that is hardly living but shows control for large conversion.[17] Livingness and control do not necessarily imply each other, and discussions of the detailed behavior were given.[17] Diagrams such as that given in Figure 5 should be very useful for predictions or analyses of experimental results. However, it must be stressed that the construction based on eqs 28−30 holds only for ideal cases of a spontaneous evolution of the persistent radical effect without any initial excess of the persistent species and without any additional radical generation, and these are seldom found in practice.

Fukuda et al.[36b,48,49] covered a situation that is more often encountered in practical polymerizations than the previous scenario. There, transient radicals are generated not only by the dissociation of R_n−Y but also with an additional rate r. These additional radicals are provided by a deliberately added conventional initiator, by impurity derived radical sources such as peroxides, or by the autoinitiation of the monomer. Now, the kinetic equations for the radical concentrations read

$$d[R]/dt = r + k_d([I]_0 - [Y]) - k_c[R][Y] - k_t[R]^2 \tag{31}$$

and

$$d[Y]/dt = k_d([I]_0 - [Y]) - k_c[R][Y] \tag{32}$$

With the ad hoc assumption of the dynamic equilibrium (19) and $d[R]/dt \ll d[Y]/dt$, these equations were solved analytically for constant r.[36b,48,49] If r is sufficiently small, the radical concentrations are given by eq 18 and the monomer consumption is given by eq 22, as if r were zero. For larger r, the radical concentrations reach the stationary state

$$[R]_s = \left(\frac{r}{k_t}\right)^{1/2} \quad \text{and} \quad [Y]_s = K[I]_0\left(\frac{k_t}{r}\right)^{1/2} \tag{33}$$

If most of the conversion occurs in this state, the polymerization index becomes

$$\ln\frac{[M]_0}{[M]} = k_p\left(\frac{r}{k_t}\right)^{1/2} t \tag{34}$$

as for a conventional polymerization with a constant initiation rate (23). This is so because the additional radical generation stops the permanent decrease of the transient radical concentration that occurs in its absence (eq 18) and keeps the radical concentration constant at a higher level. Therefore, in comparison to the absence of any additional initiation, the conversion rate is markedly enhanced.

Recently, we explored the effects of the additional initiation in detail, and found that the conditions (20) for the existence of the equilibrium (19) must again

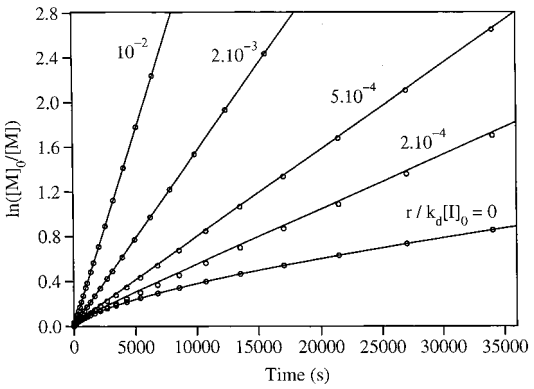

Figure 6. ln([M]$_0$/[M]) versus time for a polymerization with additional initiation and different ratios $r/k_d[I]_0$. Solid lines are from numerical calculations and circles from the analytical equations. Parameters: $k_d = 3 \times 10^{-3}$ s^{-1}, $k_c = 5 \times 10^7$ M^{-1} s^{-1}, $k_t = 10^8$ M^{-1} s^{-1}, $k_p = 2000$ M^{-1} s^{-1}, $[I]_0 = 0.1$ M, $[M]_0 = 10$ M.

be fulfilled.[50] Equations 33 are valid if $[R]_s = \sqrt{r/k_t} \gg K$, that is, the equilibrium constant must be rather small, because the radical concentrations should normally not exceed 10^{-8} M. Further, a good control and the livingness of the resulting polymer require that the rate of the cross-reaction to dormant chains largely exceeds that of the self-termination to dead products. This provides $r \ll k_d[I]_0$, which means that the rate of the additional initiation must be small compared to the cleavage rate of the dormant species. In practice, a ratio $r/k_d[I]_0 = 0.01$ yields an about 10-fold rate enhancement under retention of most of the livingness and control, but larger initiation rates should not be used if the polymer should be living at high conversion.

Figure 6 shows calculated polymerization rates ln([M]$_0$/[M]) for various ratios $r/k_d[I]_0$. Even for very small ratios of r and $k_d[I]_0$, rather large rate enhancements are obtained. Moreover, the time dependence of ln([M]$_0$/[M]) becomes linear. Since some additional initiation by impurities or autoinitiation may always occur, the nonlinear behavior for the ideal case of Figure 3 may be difficult to observe in actual polymerizations, unless $k_d[I]_0$ is sufficiently large.

The expressions for the evolution of the degree of polymerization and the polydispersity index for polymerizations in the stationary state of constant radical concentrations are[50]

$$X_n = \frac{[M]_0 - [M]}{[I]_0(1 - e^{-k_d t}) + rt} \tag{35}$$

$$PDI = (1 - e^{-k_d t} + rt/[I]_0)\left(1 + \frac{k_p}{k_d}[R]_s\frac{2 - C}{C}\right) + \frac{1}{X_N} \tag{36}$$

Here, C is the fractional monomer conversion. If one has $k_d t \gg 1$ and $rt \ll [I]_0$ at the time of observation, eq 36 reduces to

$$PDI = 1 + \frac{1}{X_N} + \frac{k_p}{k_d}[R]_s\frac{2 - C}{C} \tag{37}$$

and for small conversions, $C \approx k_p[R]_s t \ll 1$, one obtains

$$PDI_0 = 1 + \frac{1}{X_N} + \frac{2}{k_d t} \tag{38}$$

The different numerical factors (eqs 26 and 28) are due to the different time dependencies of the radical concentrations. Equation 38 has also been derived by Fukuda et al.[36b] by a purely probabilistic method, and it is generally valid for a constant concentration of growing chains.

Theoretical work has also been devoted to examine the influence of reactions that interrupt the often repeated cycles of radical formation (activation) and cross-termination to dormant species (deactivation). For the nitroxide- and the cobalt-mediated systems, such reactions are the formation of R(−H) and YH by a usual radical disproportionation, which competes with the coupling of R$^\bullet$ and Y$^\bullet$ or by a direct fragmentation of R−Y to the hydroxylamine or a hydridocobalt complex and the alkene.[22,33a,35,47,51−57] Even rather small fractions of these processes limit the maximum conversion and stop the polymerization prematurely in nearly indistinguishable ways, because they lead to an exponential decay of the dormant species. Before the end of conversion this does not affect the linear dependence of X_N on conversion and causes only minor increases of the polydispersity.[57] To some extent the deteriorating effect of these reactions can be compensated by the rate enhancement through an additional initiation.[50]

Another aspect[49] is the initial presence of persistent species in nonzero concentrations $[Y]_0$, and it will be discussed more closely in section IV. In the absence of any additional initiation, the excess $[Y]_0$ at first levels the transient radical concentration to an equilibrium value $[R]_s = K[I]_0/[Y]_0$. This is smaller than that found without the initial excess and lowers both the initial conversion rate and the initially large PDI. Further, it provides a linear time dependence of ln([M]$_0$/[M]), which is directly proportional to the equilibrium constant. Later in the reaction course, [Y] may exceed $[Y]_0$ because of the self-termination, then [R] is given by eq 18. If there is additional radical generation, the first stages will eventually be replaced by a second stationary state that was described above. Further effects are expected from a decay or an artificial removal of the persistent species that increases the concentration of the transient radicals and the polymerization rate (see section IV). Radical transfer reactions to polymer, monomer, or initiator have not yet been incorporated in the analytical treatments.

ATRP utilizes a bimolecular radical formation reaction (Scheme 14). Apart from this, the rate equations are similar to those holding for the unimolecular cases, and therefore, the theory should be similar. It is not yet far developed, but for equal initial concentrations of catalyst and initiating halide, the equations given above should also hold for ATRP with $k_d[I]_0$ replaced by $k_a[Cat]_0[RHal]_0$.[16]

3. Experimental Verifications

Stringent quantitative verifications of the analytical equations should confirm the reaction orders with

respect to time and the initial concentrations, and they should even start from the a priori knowledge of the rate constants entering the formulas. Such verifications are emerging now. Thus, several groups measured the expected rather large concentrations of the persistent species [Y] both during nitroxide-mediated polymerizations and ATRP.[31,49,58,59] Very often, the observed time dependencies of $\ln([M]_0/[M])$ were not curved as in Figure 3 but linear or approximately linear. This points to constant transient radical concentrations that are expected for an extra radical generation, an initial excess of the persistent species, or its decay. The slopes provide $[R]_s$ via eq 34. With $[R]_s$, [Y], and the initial concentrations, the equilibrium constants of the reversible radical formation can then be extracted from the data.

Fukuda et al.[49] introduced a chromatographic method for the direct determination of rate constants for the radical generation step (activation). For several cases these agree with corresponding values deduced from the time dependence of the polydispersity index (eq 38), and this is also strong support for the underlying theoretical principles. When K is known, the rate constant for radical formation (activation) provides also the rate constant for the cross-reaction (deactivation). All data established for nitroxide-mediated polymerizations so far[49,59,60,61] are not much different from rate constants for analogous reactions involving small carbon-centered radicals that have been obtained by spectroscopic techniques.[62,63] The technique has also been applied to ATRP systems.[64]

As indicated earlier, the unusual time dependencies and reaction orders expected in the absence of additional radical generation or of an initial excess of the persistent species are difficult to observe unless special precautions are taken. Moreover, a decrease of the self-termination rate constant k_t with increasing chain length and conversion diminishes the negative curvature of $\ln([M]_0/[M])$ (eq 22),[17] and may lead to a more linear appearance. This was demonstrated first by Matyjaszewski.[46] To avoid such interferences, experiments designed to prove the unusual polymerization kinetics must be based on systems that exhibit large radical generation (activation) rates, and the conversions should be kept modest. The cleavage rate constants of di-*tert*-butylnitroxide (DBNO, **1** in Scheme 12) based alkoxyamines are known to be rather large. In fact, using a sugar-carrying styrene that does not readily undergo autoinitiation and a benzoyloxy-styryl-DBNO initiator, Fukuda et al. found that the polymerization index increases with time as $t^{2/3}$ and depends on the third root of the initiator concentration.[19] This is as expected from eq 22. Other nitroxides that provide large cleavage rate constants are becoming available now (see below), and with a corresponding alkoxyamine, Lacroix-Desmazes et al. also obtained a clear verification of the theoretical predictions.[60,65] For ATRP, an example was given by Klumpermann et al.[66]

These measurements provide the equilibrium constant K of the reversible dissociation, if k_t is known. Of course, it would be interesting to obtain both

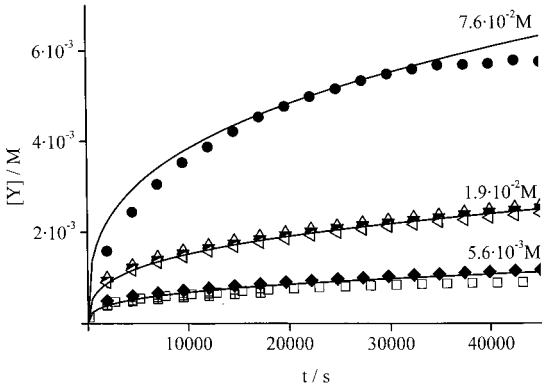

Figure 7. Time evolution of the persistent radical concentration during a polymerization of 0.76 M styrene in *tert*-butylbenzene at 130 °C initiated by the alkoxyamine **6** of Scheme 30 for different alkoxyamine concentrations. The solid lines confirm eq 18.

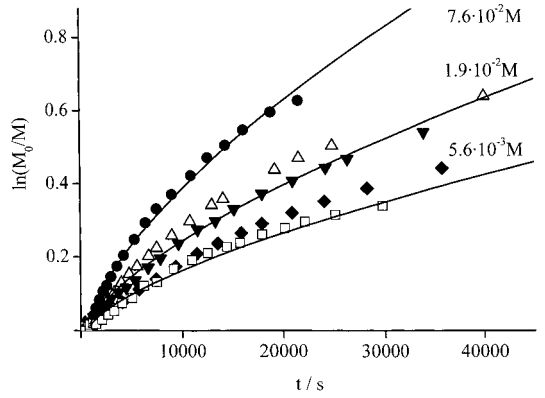

Figure 8. Time evolution of the polymerization index $\ln([M]_0/[M])$ during a polymerization of 0.76 M styrene in *tert*-butylbenzene at 130 °C initiated by the alkoxyamine **6** of Scheme 30 for different alkoxyamine concentrations. The solid lines confirm eq 22.

parameters from the same polymerization, and this is possible by simultaneous measurements of the time dependence of the persistent radical concentration and of the conversion and the combination of eqs 18 and 22.[59] This was recently achieved on the same sample by combining an ESR spectrometer with a dilatometer and using another new alkoxyamine for the polymerization of styrene. In pure monomer, the autopolymerization still provided a constant nitroxide level and a linear time dependence of $\ln([M]_0/[M])$. However, with styrene diluted by an inert solvent and for conversions below 50%, the results of Figures 7 and 8 were obtained, and they conform to eqs 18 and 22. Moreover, the resulting polymers were living (>90%) and had low polydispersities (1.15−1.30).[23]

Before closing this section, it must be mentioned that processes involving the persistent radical effect are not the only way to obtain living and controlled polymerizations. Any reaction scheme that provides an equilibrium between the dormant polymer chains and the transient propagating radicals suffices, if the equilibrium highly favors the dormant chains and is established rapidly and the rate of external radical generation is small. For such other living radical polymerizations, the RAFT process of Rizzardo et al.[67] and the moderation by degenerative iodine atom transfer[68] are illuminating examples.

III. Reactions Exhibiting the Persistent Radical Effect

A. Uncatalyzed and Photochemical Organic and Metal–Organic Reactions

The persistent radical effect must always play a role when transient and persistent radicals are formed with equal or nearly equal rates. It leads to the formation of the mutual reaction products in high yields and to the virtual absence of the self-termination reactions. In the few examples given earlier, the persistent species were radicals and transition metal complexes, but other reaction partners such as molecular ions and even normal molecules may take their place. Furthermore, the phenomenon can also work with other transient species, such as carbenes, nitrenes, and molecules in electronically excited states. A literature search would probably reveal a large variety of diverse reactions that exhibit the effect to some degree, although this went unnoticed, so far. Here, we restrict the survey to evident cases. A few of the reactions have even been designed to exploit the persistent radical effect in synthesis.

1. Photochemical Reactions Involving NO

There are a variety of photochemical reactions involving free nitrous oxide (NO) as persistent radical. Often there is an initial fragmentation, as presented in Scheme 6 for *N*,*N*-dimethyl-*N*-nitrosamine. One example is the Barton reaction of nitrite esters (Scheme 15). It allows the functionalization of methyl groups in steroids and utilizes an intermediate 1,5-hydrogen atom migration, which converts the initially formed oxygen-centered radical to a carbon-centered species.[69]

Similar reactions occur with *N*-nitrosoamines R_2-NNO and *N*-nitrosoamides RCO(R′)NNO.[70] Apart from the intramolecular hydrogen atom transfer, diverse intramolecular radical additions (cyclizations) and other rearrangements have also been used to obtain cross-reaction products between NO and the radicals resulting from the transformation of the primarily formed R• to another radical R′•.[69,70] Giving evidence for the persistent radical effect, the yields of the desired products are large and those of the self-termination of the transient intermediates are low, although these products have occasionally been observed. The photooximation of alkanes with NOCl follows essentially the same course and has industrial importance (Scheme 16).

Scheme 15

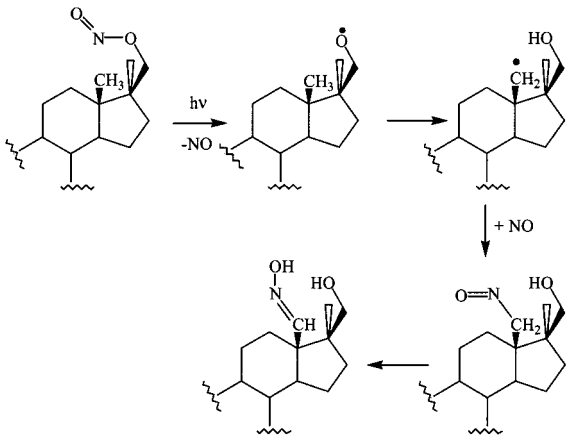

Scheme 16

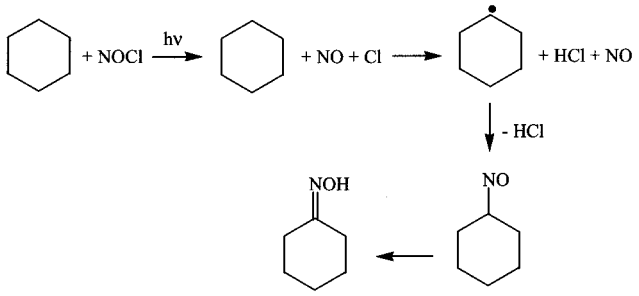

2. Thermal Reactions Involving Persistent and Semipersistent Organic Radicals

Scheme 17 displays several radicals with lifetimes exceeding about 1 h in oxygen-free liquid solutions and at ambient temperature. Many of them have been isolated in pure form.[71] Their stability has electronic and steric reasons. It is favored by the absence of β-hydrogen atoms, which would facilitate disproportionation. As shown before, the persistent radical effect can also be observed for radicals that are not extremely persistent. Therefore, it is important to notice that the lifetimes of all types of radicals can be adjusted by proper substitution.[1] Comprehensive compilations of the magnetic properties[72] and of the reactivities[73] of radicals are available in the Landolt–Boernstein series. They reveal that a large variety of radicals are persistent enough for eventual synthetic applications using the effect.

The selecting influence of triphenylmethyl radicals on product distributions has already been discussed in earlier sections, and additional examples are found

Scheme 17

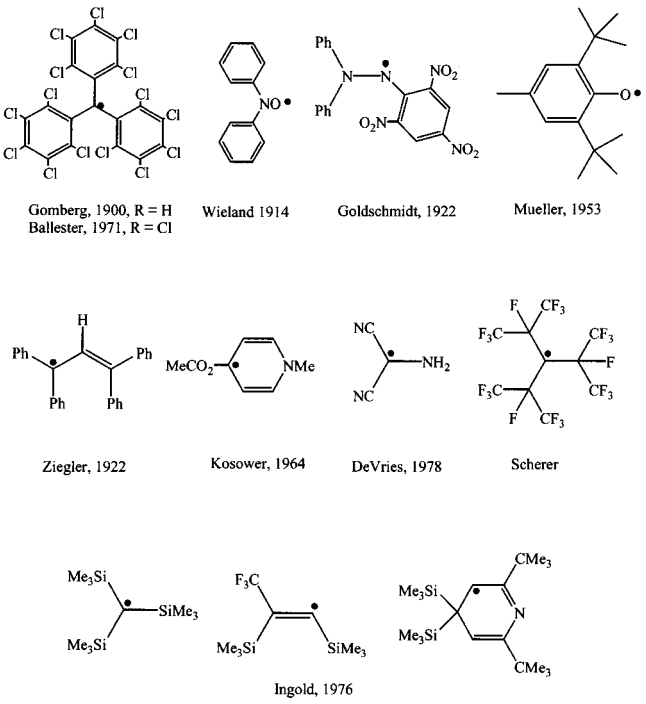

Scheme 18

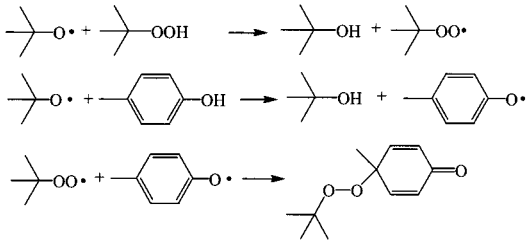

Scheme 19

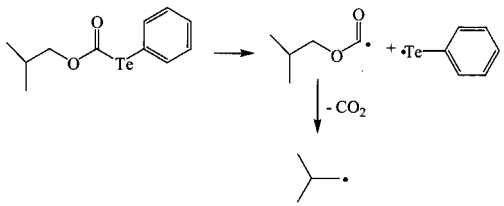

in Perkin's discussion of aromatic substitutions.[9] Minisci et al.[74] and Ingold et al.[75] found that mixed peroxide products dominate in reactions where *tert*-butylperoxy and phenoxyl or carbon-centered radicals are formed simultaneously, and the findings were rationalized in terms of the reactions shown for one example in Scheme 18.

In this case, the *tert*-butylperoxy radicals are the more persistent species. The authors also confirmed that the highest yield of the cross-reaction product is obtained when the cross-reacting radicals are formed with equal rates. Schiesser et al.[76] introduced phenyl telluroformates as precursors of alkyl radicals (Scheme 19). In the absence of trapping agents, the parent molecules appeared stable, that is, the cross-reaction between the oxyacyl and the tellurium-centered radical is even faster than the decarboxylation of the oxyacyl species, which normally takes only nano- to microseconds. Obviously, the tellurium-centered radical must be rather persistent and builds up in large concentrations.

Other reactions that are very likely subject to the persistent radical effect are molecular rearrangements such as the Meisenheimer, amineimide, Wittig, Stevens, and sulfenate rearrangements of Scheme 20, for which evidence for radical intermediates has been accumulated.[77]

The formation of pinacols, typical radical rearrangements, and the direct observation of ketyl radicals by ESR spectroscopy strongly indicate that Grignard reactions of aryl ketones follow at least in part a single electron-transfer pathway involving transient alkyl and persistent arylketyl radicals (Scheme 21). Walling[78] analyzed the known product distributions by a kinetic treatment with the ketyl species as being persistent. Most of the experimental findings were explained in terms of usual bulk radical reactions with reasonable rate constants. The operation of the effect should cause rather large concentrations of the ketyl radical species, and these are in fact observed.

Sawaki et al.[79] recognized that the persistent radical effect properly explains the dominant formation of diphenylmethyl anions when persistent dicyanoanthracene anions and transient diphenylmethyl

Scheme 20

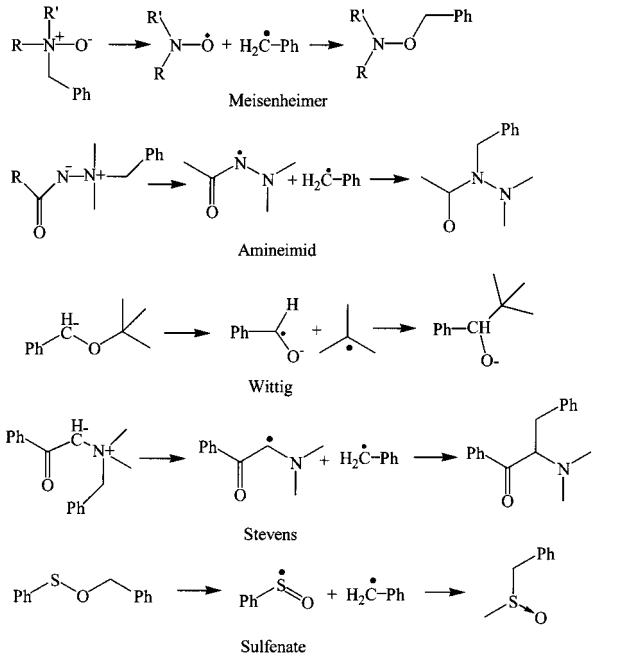

Scheme 21

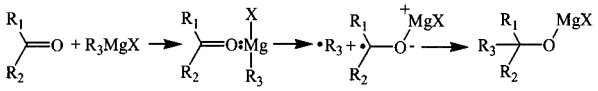

Scheme 22

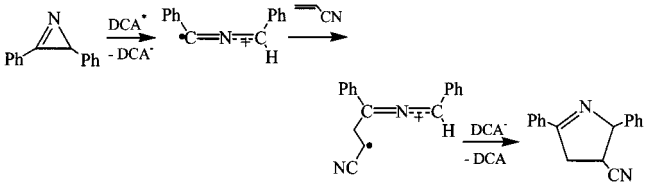

radicals are formed by photochemical means simultaneously, and they noticed the virtual absence of the coupling products of diphenylmethyl. There are a multitude of photochemical reactions involving single-electron transfer to dicyanoanthracene, dicyanonaphthalene, and related sensitizers that yield persistent anions and transient radicals simultaneously. They often lead to selective product formation and may well involve the effect.[80] Scheme 22 presents an example.[80a]

The first directed application of the phenomenon toward high-yielding organic synthesis is due to Studer.[4,81] He employed the reversible dissociation of alkoxyamines for the generation of cyclized derivatives to avoid the usual use of tin−organic compounds in radical cyclizations. One example is shown in Scheme 23.

The straightforward mechanism starts with the cleavage of the parent alkoxyamine to the nitroxide and to the 1-phenylhexen-5-yl radical. This radical undergoes intramolecular 1,5- and 1,6-cyclizations in usual ratios and couples with the nitroxide to the rearranged species. In a large series of experiments, Studer[81] made good use of the rate enhancement of the alkoxyamine cleavage by substituents stabilizing the resulting carbon-centered radicals, by polar sol-

Scheme 23

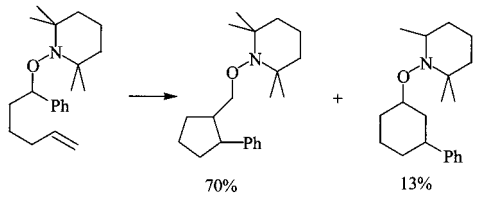

vents, and by solvents and substituents that undergo hydrogen bonding to the nitroxide group as well as by agents that decrease the retardation by slowly removing the excess nitroxide concentration. Crossover experiments demonstrated the absence of cage reactions, and several new alkoxyamines were developed that undergo a particularly facile cleavage.[81,82] It is also noteworthy that Studer often observed considerable amounts of alkenes besides the desired products. This points to the direct elimination of alkenes from the alkoxyamines, which competes with their cleavage into radicals.

3. Reactions Involving the Reversible Cleavage of Weak Metal–Carbon Bonds

In connection with the work of Kraeutler,[11] Finke et al.,[21] and Wayland et al.[37] on reactions involving the homolysis of carbon−cobalt bonds, the operation of the persistent radical effect has already been addressed. There is considerable literature on the synthetic applications of this photochemically and thermally facile process, and we refer to reviews.[83]

Scheme 24 displays an example designed by Giese et al.[84] The glycosyl−cobalt complex dissociates and the glycosyl radical adds to styrene. This adduct couples to the cobalt(II) species. The coupling product is not isolated and forms mainly the alkene by a formal "dehydrocobaltation". The alkane probably stems from a heterolytic cleavage to a radical anion and a cobalt(III) complex, followed by protonation or a direct protonation of the coupling product because this pathway dominates for electron deficient substrates.

Considerable insight into the thermodynamics, kinetics, and mechanisms associated with the reversible cleavage of weak metal−carbon, metal−hydrogen, and metal−metal bonds is due to Halpern.[85] Scheme 25 shows the major reactions in liquids. The thermal cleavage is believed to produce a caged

Scheme 24

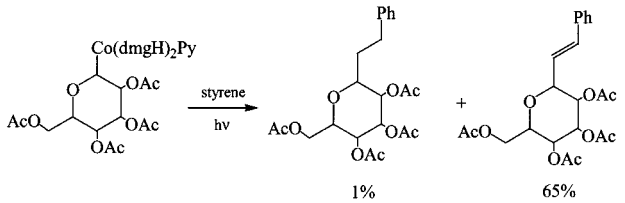

Scheme 25

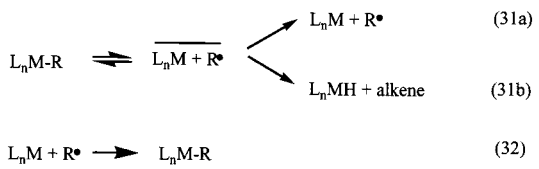

Scheme 26

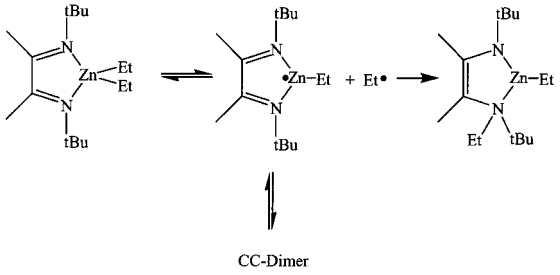

radical pair that undergoes cage return and separation to scavengeable free radicals and forms alkenes by disproportionation. The recombination of the radicals from the bulk is close to diffusion-controlled and does not seem to be accompanied by disproportionation. In usual free radical reactions, disproportionation-to-combination ratios in bulk and cage are often equal. Therefore, the marked difference observed here for the postulated cage return and the bulk process is against the former reaction. In our opinion it is more compatible with an alkene formation by direct elimination from the initial complex. However, this was regarded to be unlikely,[85] and unusual coordination effects may be involved.

Halpern noticed the relevance of the reactions of Scheme 25 in biological coenzyme B_{12}-mediated rearrangements, and the use of vitamin B_{12}-promoted radical reactions in organic synthesis was pioneered by Scheffold.[86] The latter reactions are often carried out in electrochemically driven catalytic cycles where the operation of the persistent radical effect is not evident.

Most of the synthetic literature concerns the utilization of the weak cobalt−alkyl bonds. However, the reversible cleavage into transient radicals and a metal complex residue is also known for many other complexes, for example, those of Ti, V, Cr, Mn, Fe, Ni, Cu, Zn, Zr, Mo, Ru, Rh, W, U, Pb or the lanthanides Sm, Ir, Sc, Hf, Th, etc.[83c,85,87] Some of them are of synthetic use, and many metal species may be persistent. Hence, the persistent radical effect should be operating. Van Koten[88] has presented a clear-cut example (Scheme 26). Et_2Zn reacts with di-*tert*-butyl-glyoxaldiimine to a complex that rearranges in nearly quantitative yield by a 1,2-ethyl migration from Zn to nitrogen. The organozinc radical is persistent and forms a weakly CC-bonded dimer. The reaction works at low temperatures, with diversely substituted diimines and α-imino ketones, and with $AlEt_3$ as inorganic precursor and has been used in synthetic applications.

B. Catalyzed Organic Reactions

1. Catalyzed Kharasch Additions and Related Reactions

The discovery of Minisci et al.,[39] Asscher and Vofsi,[40] and others[41] of the transition metal catalyzed addition of haloalkanes to alkenes by a redox chain process (Scheme 14) has found vast synthetic applications.[83c,89] A recent summary has been given by van Koten et al.[90] Virtually any olefin can serve as the source of reactive unsaturation, and a variety of polyhalogenated compounds such as alkyl halides,

Scheme 27

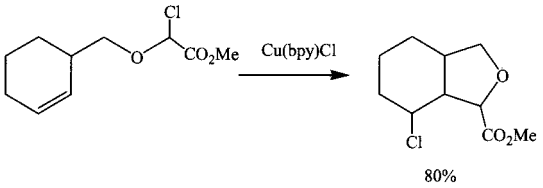

Scheme 28

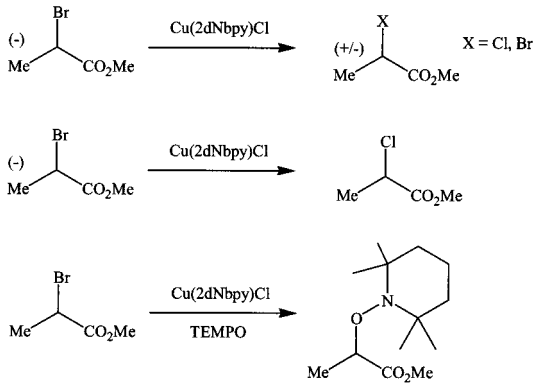

perfluoroalkyl iodides, or alkylsulfonyl chlorides can be added across the double bond. The list of the catalytic promotors is extensive. It includes powdered transition metals; their inorganic oxides or halides with the metal in a lower valent state; mono-, di- and trinuclear transition metal complexes with various organic ligands; and metal phosphine compounds such as $RuCl_2(PPH_3)_3$. Telomerization is normally avoided by using large ratios of the halogenated compounds to the olefin but has also found synthetic interest.[89b] More recently, the reaction has been used to obtain radical cyclization products in excellent yields,[91] as for example outlined in Scheme 27.[91b]

Because of the excellent yields, the intermediacy of freely diffusing carbon-centered radicals in these reactions has often been doubted. However, the identical product distributions of the same cyclizations carried out by transition metal catalysis and by conventional radical reactions point to the opposite.[91b] Even stronger experimental evidence for normal uncomplexed free radical intermediates has recently been given by Matyjaszewski et al.[92] This group studied three reactions of methyl 2-bromopropionate with copper(I) chloride complexed by 4,4′-di-(5-nonyl)-2,2′-bipyridine (dNbpy) under identical conditions. These were (Scheme 28) the racemization of an optically active propionate, the exchange of Br by Cl, and the trapping of the radical intermediate by excess TEMPO. Both the rates and yields of all three reactions were identical. This is only expected if free 1-carboxymethyl-substituted ethyl radicals are the common intermediates, and the rates reflect the rate of radical formation. The observations rule out major contributions by reactions in the metal coordination sphere. In all catalyzed reactions, large concentrations of the persistent metal complexes in the higher valent state should be reached, and these were in fact also observed occasionally.[58,90]

Generally, the reaction rates increase strongly with the decreasing oxidation potential of the complex, and these can be tuned by appropriate ligands. These ligands also provide the solubility of the complexes and exert additional steric effects. Moreover, the activation of the halide substrate plays an important role. We refer to a collection of relevant references.[90]

2. Photocatalysis

Photochemical reactions of polyoxymetalate anions, such as tetrakis(tetra-*n*-butylammonium)decatungstate $(C_4H_9N)_4W_{10}O_{32}^{4-}$, have been used for the catalytic ethylation, vinylation, carbonylation, and hydroperoxidation of alkanes in liquid solution.[93] The simplest mechanism of Scheme 29 involves the reversible formation of a paramagnetic decatungstate species and a transient radical. As proven by optical and EPR spectroscopy, the decatungstate intermediate is persistent.[94] Moreover, during continuous photoreactions in the presence of a large variety of differently substituted alkanes, the concentration of the decatungstate intermediate exceeded the concentrations of the transient radicals by factors of 100−5000. In pulsed radical generations, the transient species decayed completely after the pulse, whereas residual reduced decatungstate remained. This is experimental proof for the persistent radical effect in these systems and allowed the determination of reaction rate constants.[94]

Scheme 29

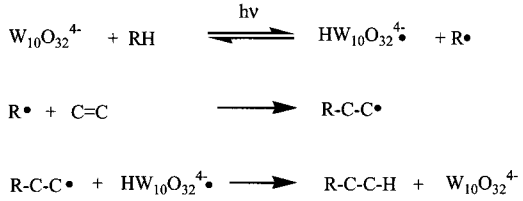

C. Reactions in Polymer Systems

For more complete and practically oriented surveys of living radical polymerizations, we refer to other reviews in this issue[95] and cover in the following section only some kinetic and mechanistic aspects that are relevant for quantitative treatments.

1. Nitroxide-Mediated Systems

The rate constants of the cleavage of the dormant chains into radicals (activation) and of the reverse coupling (deactivation) influence the degree of livingness and control of the resulting polymer and the monomer conversion rate. To obtain living and well-controlled radical polymerizations, these rate constants must favorably interrelate with the propagation constants k_p and the termination constants k_t of a particular monomer system at a given temperature, as well as with the applied initiator (regulator) concentration $[I]_0$ and the rate r of an additional radical generation. For systems involving the reversible bond cleavage, we have denoted the activation and deactivation parameters by k_d and k_c (Scheme 8), and their ratio $k_d/k_c = K$ is the equilibrium constant. The knowledge of these quantities and of the factors controlling them allows the preassessment of successful processes.

The alkoxyamines presented in Scheme 12 were used as regulating initiators early on,[27] and Scheme

Scheme 30

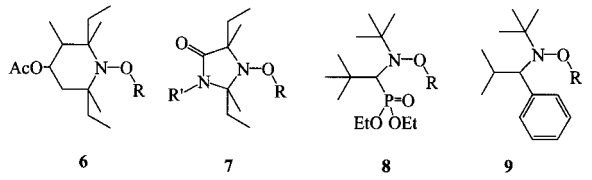

6 7 8 9

30 lists a few advanced species.[60,96−98] Alkoxyamines are usually prepared by the coupling of suitable carbon-centered radicals with the corresponding nitroxides[60,97,99−101] but can be formed also in situ during polymerizations by the Meisenheimer rearrangement of *N*-oxides[102] (Scheme 20), by sequential radical additions to nitroso compounds and nitrones,[103] by the coupling of nitroxides with radicals originating directly from conventional initiators, or from the addition of primary initiator radicals to the monomers.[30,31] Further, polymeric alkoxyamines have been used as initiators.[49] Since the free nitroxide radicals act as persistent regulating species, it is often believed that they should be fairly stable under polymerization conditions, typically up to temperatures of 130−140 °C. However, this need not be so (see section IV). Except for compounds **1**, **8**, and **9**, the nitroxides indicated in Schemes 12 and 30 are very stable. Di-*tert*-butyl nitroxide **1** slowly decomposes to *tert*-butyl radicals and nitrosobutane. The nitroxides derived from **8** and **9** presumably undergo disproportionation, but the reaction is slow because of steric constraints.[62]

TEMPO, *p*-substituted TEMPO based alkoxyamines **3**, and compounds such as **4**, **5**, and **7** have been applied successfully for polymerizations of styrene, substituted styrenes, and 4-vinylpyridine, and some copolymerizations and block copolymerizations were reported. However, living and controlled radical polymerization of other monomers, especially acrylates, require the use of the more recently developed structures **6**, **8**, or **9**. These also yield well-controlled and living block copolymers, but methacrylates have so far resisted all efforts to obtain large conversions. Undoubtedly, many failures are due to unfavorable rate constants or side reactions.

As mentioned before, the equilibrium constant K can be determined from polymerization data. For polymeric alkoxyamines (macroinitiators) k_d has mostly been determined with Fukuda's chromatographic method[49] or from the early time evolution of the polydispersity (eqs 18 or 22). From K and k_d one obtains k_c. The decay constant k_d can also be obtained from the exponential growth of the persistent radical concentration during the cleavage of alkoxyamines under conditions where the transient radicals are completely scavenged, preferrably by the irreversible reaction with another persistent radical. This technique has been widely applied to low molecular weight alkoxyamines.[22,62,104−107] The rate constants of the coupling k_c of nitroxides with small carbon-centered radicals are usually measured by laser flash photolysis.[63,108,109]

Table 1 displays rate data for alkoxyamine-terminated polymers and low molecular model compounds and shows some important trends. At about the same temperature, the dissociation rate constants k_d of alkoxyamines (Schemes 12 and 30) with the same leaving radical (polystyryl, 1-phenylethyl) increase in the order **3** (TEMPO) < **6** < **8** (DEPN) < **1** (DBNO) by a factor of about 30. Acrylate radicals dissociate markedly slower than styryl radicals from **1** (DBNO), but there is no appreciable difference for **8** (DEPN). The dependence of k_d on the nitroxide structure has been addressed by Moad et al.[104] They found the order five membered ring < six membered ring < open chain nitroxides and pointed out additional steric (compare **3** and **6**) and polar effects.

The activation energies of the cleavage are close to the bond dissociation energies and can be reliably calculated with advanced quantum chemical methods.[110] For a large series of low molecular alkoxyamines with different leaving radicals, they decrease linearly with increasing stability of the leaving radical, that is, the R−H bond dissociation energy.[62,106] Thus, k_d increases in the series acrylate < styryl < methacrylate and within one type of radical from primary to secondary and tertiary species. The frequency factors are in the rather narrow range from 3×10^{13} s^{-1} to 2×10^{15} s^{-1}, and for a larger series of

Table 1. Rate and Equilibrium Constants for the Reversible Dissociation of Polymeric Alkoxyamines and Low Molecular Model Compounds, Frequency Factors, and Activation Energies of Dissociations

alkoxyamine, Schemes 12, 30	T/°C	k_d/s^{-1}	A_d/s^{-1}	$E_{a,d}$/kJ mol^{-1}	k_c/M^{-1} s^{-1}	K/M	ref
3-(TEMPO)-polystyryl	125	0.0016	3×10^{13}	124	7.6×10^{7}	2.1×10^{-11}	48, 49
	125	0.00052			$\approx 1 \times 10^{8}$	$\approx 1 \times 10^{-11}$	31
	120	≈0.001					35
3-1-phenylethyl	120	0.00052	2.5×10^{14}	133	2.5×10^{8}	2.1×10^{-12}	62, 63
	120	0.00045	5×10^{13}	128			105
1-(DBNO)-polystyryl	120	0.042	3.8×10^{14}	120			48, 49
1-phenylethyl	120	0.014	2.2×10^{14}	122			62
1-poly-*tert*-butylacrylate	120	0.001					48, 49
1-1-*tert*-butoxycarbonylethyl	120	0.0011	1.2×10^{14}	128			62
6-polystyryl	130	≈0.0032			$\approx 6 \times 10^{6}$	5.2×10^{-10}	23
6-1-phenylethyl	120	0.0027			1×10^{8}	2.7×10^{-11}	62, 63
8-(DEPN)-polystyryl	125	0.0034	1×10^{14}	121	5.7×10^{5}	1.9×10^{-8}	65
	120	0.011	2×10^{15}	130		6×10^{-9}	59
	120						48, 49
8-1-phenylethyl	120	0.0055	1.9×10^{14}	125	4.6×10^{6}	1.2×10^{-9}	62, 63
8-poly-*n*-butylacrylate	120	0.0071	1.7×10^{15}	130	4.2×10^{7}	1.7×10^{-10}	59
8-1-*tert*-butoxycarbonylethyl	120	0.003	3.5×10^{14}	128			62

model compounds, a clustering around 2×10^{14} s^{-1} was observed. These frequency factors are remarkably small since for molecular dissociations into fairly large groups values much larger than 10^{15} s^{-1} are usual.[111] Obviously, nearly the whole bond dissociation energy is needed to reach the transition state of the cleavage while little entropy is gained. Further, we note that the cleavage is favored by polar solvents, external and internal hydrogen bonding, strong steric congestion around the NO group, increasing CNC bond angles, and electron-donating groups on the nitroxide moiety.[82,104]

The rate constants for the coupling of carbon-centered radicals with nitroxides (Table 1) range from 6×10^5 M^{-1} s^{-1} to about 10^8 M^{-1} s^{-1}, and they vary more than the cleavage rate constants. Many studies on small radicals have shown that the rate constants are generally lower than diffusion controlled values and depend very little on temperature.[63,108,109] In some cases even negative activation energies have been found, whereas the rate constants with small positive activation energies often revealed unusually small frequency factors. This is rationalized by a nearly barrierless cross-coupling reaction, where the location of the transition state is governed by entropy. Support for this explanation is the anticorrelation of the cleavage of alkoxyamines and the coupling rate constants for systems with the same basic structures but different substitutions.[63]

In total, alkoxyamine systems with large cleavage (activation) rate constants tend to show small coupling (deactivation) rate constants. This provides large equilibrium constants that increase the conversion rates. It must not deteriorate the control since this depends on k_d and the product $k_d k_c$. In comparison, the more recently introduced nitroxides **6**, **8**, and **9** provide larger equilibrium constants than e.g. **3** (TEMPO). For acrylate-derived radicals, the equilibrium constants are usually smaller than for styryl type radicals, and this may, at least in part, explain the failure of TEMPO-regulated acrylate polymerizations. However, judging from model studies,[62,63] this reason does not apply for methacrylates.

Reactions that convert the alkoxyamines to hydroxylamines and alkenes can strongly limit the monomer conversion. These are either usual radical disproportionations between the nitroxide and the propagating radicals or concerted alkoxyamine decays. Both pathways lead to an exponential decrease of the concentration of the dormant chains with rate constant $k_{dec} = f_D k_d$, where f_D is the fraction of the side reaction concurring with radical coupling of alkoxyamine decay.[57] k_{dec} can be measured from the decay of the dormant alkoxyamine chains under nonscavenging conditions, and its relation with k_d provides f_D. From data of Fukuda et al. one can deduce $f_D = 0.4\%$ for a TEMPO-polystyryl compound and $f_D = 1.1\%$ for a di-*tert*-butylnitroxide-poly-*tert*-butylacrylate macroinitiator both at 120 °C.[53,55] Similar small values of f_D hold for TEMPO-cumyl (Scheme 10),[22] TEMPO-1-phenylethyl,[112] and a better mimetic compound for TEMPO-polystyryl.[113] In these cases, f_D probably represents the usual radical disproportionation. A much larger $f_D \approx 25\%$ holds for TEMPO−$CH(CH_3)CO_2CH_3$. It is ascribed to the concerted alkene elimination, which is also known for TEMPO-alkyl compounds.[81,112] However, for TEMPO−$CH(CO_2CH_3)CH_2C(CH_3)_2C_6H_5$, the fraction of the side reaction is again low ($f_D \approx 1\%$), so TEMPO−$CH(CH_3)CO_2CH_3$ is not a good model for TEMPO-terminated acrylates. Nevertheless, one may speculate that side reactions contribute to the difficulties encountered with TEMPO-mediated acrylate polymerizations, because they are virtually absent for DEPN (**8**) based systems.[112] Similarly, the nitroxide **9** exhibits a much better end group fidelity than TEMPO in styrene and acrylate polymerizations.[114]

The irreversible decay of the dormant alkoxamine chains stops the monomer conversion rather abruptly at the time $t = 1/f_D k_d$. For methyl methacrylate polymerizations this stop has been observed, and it has been demonstrated that it is caused by a considerable fraction of cross-disproportionation between the nitroxide and the propagating radicals.[51,97,112] Unfortunately, the factors governing disproportionation-to-combination ratios in radical−radical reactions are not well understood up to now, but stereoelectronic effects are certainly very important.[112] Hence, one cannot yet predict a nitroxide structure that will allow living methacrylate polymerizations up to large conversions.

Recently, it has been found that the elimination of the hydroxylamine from a nitroxide-capped polymer occurs particularly facilely upon the controlled monoaddition of maleic anhydride and maleimide derivatives under the creation of a very useful functional end group, that is, the often detrimental side reactions can also be put to good use.[115]

A complete mechanism of the nitroxide-mediated polymerizations must also take further reactions into account. For the case of TEMPO + styrene, Scaiano et al. showed that the nitroxide radical can add directly to the monomer.[116] It can also abstract a hydrogen atom from the Mayo dimer[117] and possibly from the polystyryl chains.[116] In addition, hydroxylamines can act as hydrogen donors for the propagating radicals and retard the polymerization.[118] Quantitative assessments of the importance of these reactions are still missing, but the practical experience with living radical polymerizations points against strong deteriorating influences.

2. Mediation by Other Persistent Radicals

Most of the living radical polymerizations using organic radicals as regulating persistent species involved nitroxides. Exceptions are triphenylmethyl and other carbon-centered radicals in the early work of Otsu and Braun.[24,25] More recently, Chung showed that borinate radicals **10** formed by the thermal cleavage of in situ generated alkyl boryl peroxides (Scheme 31) can be employed to control methacrylate

Scheme 31

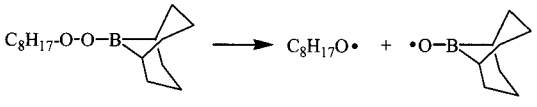

10

Scheme 32

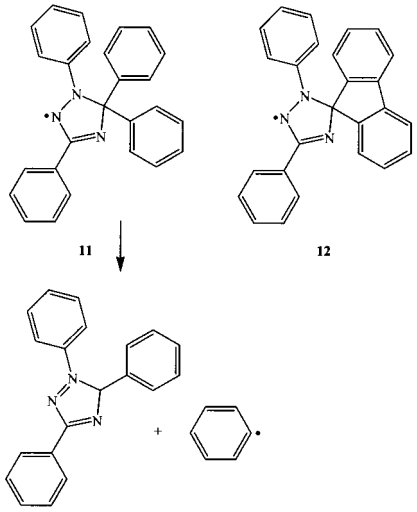

polymerizations partially.[119] Müllen et al.[120] introduced the triazolinyl radicals **11** and **12** (Scheme 32) for the regulation of styrene, acrylate, methacrylate, and vinyl acetate polymerizations and demonstrated the formation of block copolymers. At least for moderate conversions, they reported more success than obtained with the structurally related verdazyl radicals and with TEMPO.[121] It was also demonstrated that the triazoninyl radicals couple reversibly to the propagating radicals, as is known for nitroxides.

Radical **12** is rather stable under polymerization conditions, but radical **11** decays into a triazole and the phenyl radical, which initiates new chains. Hence, the rate of polymerization is higher with **11** than with **12**, because the decay prevents retarding of the buildup of large persistent radical concentrations such as an additional radical generation. This effect of the radical decay is equivalent to the rate enhancement by partial removal of nitroxides by appropriate additives, which was first applied by Georges et al.[31] Interestingly, at 95 °C and in toluene solution, the lifetime of **11** is only about 15 min, whereas a reasonable control was found in polymerizations of styrene that lasted many hours at 120−140 °C.[120] Obviously, the radical moiety **11** is stable while it is coupled to the polymer chain. However, the different time scales raise the question of the upper limit of the conversion rate of the persistent radical to a transient one that can be tolerated in living radical polymerization processes (see section IV.C).

3. Organo–Cobalt Complex Mediated Systems

A kinetic study of living radical polymerizations of acrylates initiated by the (tetramesitylporphyronato)-cobalt(III) organo complexes (TMP)Co−$CH(CH_3)CO_2$-Me and (Br_8TMP)Co−$CH(CH_3)CO_2$Me has been reported by Wayland et al.[122] They applied an initial excess of the free cobalt complex and obtained the equilibrium constant for the reversible dissociation of the complex−poly(methyl acrylate) bond as $K = 4.2 \times 10^{-10}$ M for (TMP)Co and $K = 1.3 \times 10^{-8}$ M for (Br_8TMP)Co from the rate of monomer consumption at 50 °C. The temperature dependence led to a bond dissociation energy of 100 kJ mol^{-1} for (TMP)Co−poly(methyl acrylate). In comparison with the data given for higher temperatures in Table 1, the equilibrium constants are considerably larger than for the alkoxyamines. The coupling reaction between cobalt complexes and carbon-centered radicals is often diffusion controlled,[85] and hence, the bond dissociation energy of 100 kJ mol^{-1} should be close to the cleavage activation energy. For alkoxyamines, the activation energies are larger. Obviously, the cobalt-complex-mediated acrylate polymerization is favored by the weak metal−alkyl bond, and the dissociation constants k_d of the complexes must be on the order of 10^{-2}−1 s^{-1}. The frequent "dehydrocobaltation" to a hydridocobalt complex and an olefin[85] seems to be of minor importance for acrylates, but it may have precluded other cobalt-complex-mediated polymerizations.

4. Atom Transfer Radical Polymerization

In comparison to the nitroxide- and cobalt-mediated processes, atom transfer radical polymerizations are mechanistically more complex. Thus, the catalyst reactivity depends on the ligand, the counterion, the transition metal itself, and the initiating organic halide. Moreover, it is possible that more than one unique catalytic species is involved, and structural investigations are still scarce.[123] So far, copper-based systems seem to be the most efficient[124] when compared to other transition metals such as iron,[125] nickel,[126] ruthenium,[42] rhodium,[127] or palladium.[128] The counterions are often chloride and bromide, and bromide normally yields higher rates. As initiators one uses compounds that structurally resemble the chain ends of the dormant chains, that is, for example, α-bromoisobutyrates [$(CH_3)_2CBrCO_2Me$] for methacrylates, α-bromopropionates ($CH_3CHBrCO_2$-Me) for acrylates, and 1-bromoethylbenzene [C_6H_5-$CH(CH_3)Br$] for styrene, but aromatic sulfonyl chlorides are also quite versatile.[44,129] A large variety of complexing ligands has been applied,[130−136] and Scheme 33 lists a few bi-, tri- and tetradentate nitrogen-based systems for the complexation of copper ions. In general, the activity decreases in the order of the ligands alkylamine ≈ pyridine > alkyl

Scheme 33

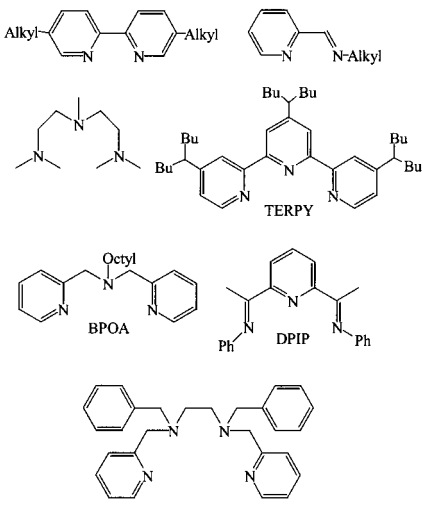

imine ≫ aryl imine > arylamine,[134] and tris(2-(dimethylamino)ethyl)amine seems to be one of the most efficient ligands.[124]

Atom transfer polymerizations are often subject to problems arising from solubility, the initial presence of metal ions in the higher oxidation state, multiple complex equilibria, and a variety of side effects.[137−139] Quite often, diverse broken reaction orders are observed with respect to catalyst and initiator, and they are difficult to analyze.[140] Nevertheless, with the methods outlined above for nitroxides, some quantitative data for the reversible radical formation steps were obtained.

Table 2 shows results for polymeric and low molecular model systems. If one takes the second-order radical formation into account and assumes 0.1 M concentrations of initiator and catalyst, the atom transfer favors the radical formation (activation) more than the alkoxyamine dissociation. On the other hand, the cross-reaction rate constants k_c and k_{deact} show similar orders of magnitude for both types of reactions. This explains the generally shorter reaction times for the metal-catalyzed systems. In model studies Matyjaszewski et al.[134] found that the rate constant k_{act} for radical formation from Cu(I) complexes and organobromides increases with decreasing reduction potential of the complex and can be tuned by the choice of the ligand. This is also known in organic synthesis (see above) and it points to an activation-controlled forward reaction. The authors also noticed an anticorrelation between k_{deact} and k_{act}, that is, larger rate constants for the radical formation parallel the smaller rate constants for the reverse reaction. The same holds for the nitroxide-based systems, and it may indicate an entropy-controlled deactivation. If this is generally true, one expects only weak or even negative temperature dependencies of k_{deact}.

IV. Theoretical Methods and Special Cases of Living Radical Polymerizations

A. The Basic Reaction Mechanism

In this section we summarize a method for the quantitative treatment of living radical polymerizations involving the persistent radical effect. It is quite general and can be applied to many cases. We start with the minimum mechanism given in Scheme 3 and the assumptions stated earlier. The concentrations of the radicals R• and Y• obey

$$d[R]/dt = k_d[I] - k_c[R][Y] - k_t[R]^2 \quad (39)$$

$$d[Y]/dt = k_d[I] - k_c[R][Y] \quad (40)$$

By stoichiometry, they are related by $[I]_0 - [I] = [Y] = [R] + [P]$. Hence, [I] can be expressed by [Y], and the concentration [P] of the termination products is practically equal to the concentration of the persistent species [Y].

According to the rate equations (39 and 40), both radical concentrations increase at first linearly with time as $[R] = [Y] = k_d[I]_0 t$, and they attend a stationary state only at infinite time, where $[Y]_\infty = [P]_\infty = [I]_0$ and $[R]_\infty = 0$, that is, when the initiator is fully converted to persistent radicals and unreactive products. To find the intermediate behavior and the dynamic equilibrium, we cast the rate equations into simpler forms by using reduced variables and parameters

$$\rho = \frac{[R]}{[I]_0} \quad \eta = \frac{[Y]}{[I]_0} \quad \tau = k_d t \quad a = \frac{k_c[I]_0}{k_d} \quad b = \frac{k_t[I]_0}{k_d} \quad (41)$$

and the definition $\dot{x} = dx/d\tau$. This yields

$$\dot{\rho} = 1 - \eta - a\rho\eta - b\rho^2 \quad (42)$$

$$\dot{\eta} = 1 - \eta - a\rho\eta \quad (43)$$

Obviously, the kinetics are determined by two parameters, a and b, only. It is thus sufficient to solve the differential equations in terms of a and b and then go back to the real concentrations and times via the relations 41.

The parameters a and b depend on $[I]_0$, and the rate constants and their magnitudes can be estimated. In polymerizations, one often aims at average degrees of polymerization of 100−1000 for an initial monomer concentration of about 10 M (bulk). Hence, one uses $[I]_0 = 10^{-2}-10^{-1}$ M. For small radicals R• and low viscosities, the termination constant is

Table 2. Rate and Equilibrium Constants for the Reversible Bromine Atom Transfer Reaction of Polymeric and Low Molecular Model Compounds with Cu−Complexes. For Ligand Structures, See Scheme 33

initiator or dormant chain	catalyst	T/°C	k_{act}/M^{-1} s^{-1}	k_{deact}/M^{-1} s^{-1}	K	ref
poly(methyl methacrylate)−Br	CuBr/(4,4-di-*n*-heptyl-2,2-bipyridine)$_2$	100			7×10^{-7}	124
ethylisobutyrate−Br	CuBr/TERPY	35	1.5			132
	CuBr/BPOA	35	0.3			132
	CuBr/DPIP	35	0.1			132
polystyryl−Br	CuBr/(4,4-di-*n*-heptyl-2,2-bipyridine)$_2$	110	0.45	1.1×10^7	3.9×10^{-8}	64, 131
		90			2×10^{-8}	64, 131
1-bromoethylbenzene	CuBr/TERPY	35	0.42	4.1 ×105 [a]		132
	CuBr/BPOA	35	0.066	3.3×10^6 [a]		132
	CuBr/DPIP	35	0.014	3.1×10^6 [a]		132
poly(methyl acrylate)−Br	CuBr/(4,4-di-*n*-heptyl-2,2-bipyridine)$_2$	90			1.2×10^{-9}	131
methyl proprionate−Br	CuBr/(4,4-di-*n*-heptyl-2,2-bipyridine)$_2$	60	0.065			92
	CuBr/TERPY	35	0.41			132
	CuBr/BPOA	35	0.014			132
	CuBr/DPIP	35	0.011			132

[a] 75 °C.

usually $k_t \approx 10^9$ M^{-1} s^{-1}, and it reduces to 10^7-10^8 M^{-1} s^{-1} for long chains. For the special case of alkoxyamines, the cross-coupling rate constants are in the range $k_c = 10^5-10^8$ M^{-1} s^{-1}, and k_d ranges from 10^{-5} to 1 s^{-1} for reaction temperatures around 120 °C (Table 1). This places a between 10^3 and 10^{14} and b between 10^5 and 10^{14}. Hence, a and b are always large compared to 1, and one also expects $a^2/b \gg 1$ for most individual cases.

The system of nonlinear differential equations 42 and 43 has no closed solution. Our analysis starts from an investigation of the possible trajectories of the point $(\rho(\tau),\eta(\tau))$ in the two-dimensional phase plane spanned by the variables ρ and η. These are limited by stoichiometry to values between 0 and 1. Moreover, from eqs 42 and 43 one has

$$\dot{\eta} = \dot{\rho} + b\rho^2 \tag{44}$$

For the given initial conditions this implies that $\eta \geq \rho$ for all times. Hence, all trajectories are in the plane $(0,1) \times (0,1)$, start at the origin (0,0) along the first diagonal and then deviate positively therefrom. Setting $\dot{\eta} = 0$ and $\dot{\rho} = 0$ in eqs 42 and 43 yields the singular point (0,1) at infinite time.

In the intermediate time regime, the evolution of the trajectories follows from the behavior of isoclines, where the time derivatives of the dynamic variables are individually zero, namely isocline $\eta_1(\rho)$, where $\dot{\rho} = 0$, and isocline $\eta_2(\rho)$, where $\dot{\eta} = 0$. From eqs 42 and 43 these are

$$\eta_1(\rho) = \frac{1}{1 + a\rho} \quad \text{and} \quad \eta_2(\rho) = \frac{1 - b\rho^2}{1 + a\rho} \tag{45}$$

The isoclines divide the phase plane into regions of different signs of the time dependencies of ρ and η, as is indicated in Figure 9 in a log−log representation. Consequently, any trajectory can cross the isocline η_1 only horizontally and in the direction of decreasing ρ, and it can cross the isocline η_2 only vertically in the direction of increasing η. Further, η_2 crosses the line $\eta = 0$ at the maximum $\rho = 1/\sqrt{b}$, and both isoclines approach the final point (0,1) with the same slope.

Figure 9 also shows a computed trajectory for the parameters $(a, b) = (10^8, 10^8)$. After the initial increase along the first diagonal, the trajectory bends up and crosses the isocline η_2 vertically. Thereafter, ρ decreases and η continues to increase. The trajectory cannot cross η_2 a second time, since it must do so vertically in the direction of increasing η. It cannot cross the isocline η_1 either, since it must do so horizontally in the direction of decreasing ρ. Therefore, after the first crossing, the trajectory is confined to the region between the two isoclines. This region is very narrow for the chosen parameters. Staying between the isoclines, the trajectory finally approaches the final point. The maximum of ρ is on isocline η_2. Therefore, ρ is limited to values below $\rho = 1/\sqrt{b}$.

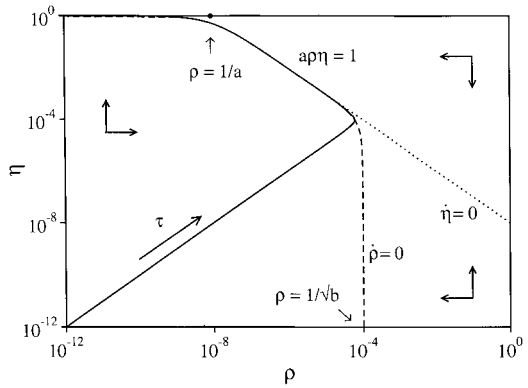

Figure 9. Trajectory of the point (ρ,η), that is, the reduced concentrations of the radicals R• and Y•, and the isoclines $\dot{\rho} = 0$ (dashed) and $\dot{\eta} = 0$ (dotted) in the phase plane and in a log−log representation. Parameters $(a, b) = (10^8, 10^8)$.

In the log−log representation of the phase diagram, the dynamic equilibrium relation 19 (k_c[R][Y] = k_d[I]$_0$) or $a\rho\eta = 1$ appears as a straight line with slope −1. It starts at $(\rho, \eta) = (1/a, 1)$, and it is practically identical to η_1 for $\rho > 1/a$. The trajectory must closely follow η_1, and hence, there is a time range where the equilibrium relation is certainly valid. With increasing $1/a$, the equilibrium line shifts to the right. It will not be reached at all when $1/a$ becomes close to $b^{-1/2}$. Consequently, one condition for the existence of the equilibrium is $a^2/b \gg 1$. Further, because $\rho < 1$, one has $b \geq 1$, and this implies the third condition $a \gg 1$ by combination with the first. With the definitions 41, this yields eqs 20.

In the transition region between the initial and the equilibrium regime, the details of the time evolutions are complicated.[17] However, for the equilibrium regime where $a\rho\eta = 1$, the integration of eq 44 leads to eqs 18.[17] These solutions are obeyed until η approaches 1 and ρ approaches $1/a$, and this happens at the approximate time $t = [I]_0/3K^2k_t$. For nitroxide-based systems with a large equilibrium constant, $K = 10^{-8}$ M (Table 1), a rather small initiator concentration, $[I]_0 = 10^{-2}$ M and $k_t = 10^8$ M^{-1} s^{-1}, the equilibrium, and that is also the persistent radical effect, lasts for about 90 h, and it is entered at rather short times of at most seconds.[17]

Polymerizations are studied typically in time ranges between 100 s and 30 h, that is, in the equilibrium regime. Therefore, for polymerizing systems, one can use eq 20, insert it into the rate equation of the monomer consumption (21), integrate, and obtain eq 22. The further derivation of the control involves the calculation of the moments m_k of the chain length distribution and of their time dependencies.

$$m_k = \sum_{n=1}^{\approx} n^k([I_n] + [P_n] + [R_n]) \quad k = 0, 1, 2$$

The exclusion of $n = 0$ in the summation ensures that only monomer-containing species are counted, because we start from a monomer-free initiator. If a monomer-containing initiator would be used, the zeroth moment m_0 would be equal to $[I]_0$, because of the stoichiometry relations. Hence, one has in our case

$$m_0 = [I]_0 - ([I_0] + [P_0] + [R_0]) \tag{46}$$

where $[I_0]$, $[P_0]$, and $[R_0]$ are the concentrations of the

initiator, the transient radicals, and the products that do not contain monomer units. It seems reasonable to assume and is borne out by numerical calculations that $[I_0]$ decays exponentially because $R_0^\bullet$ immediately adds to the monomer. For the same reason, $[R_0]$ and $[P_0]$ are small compared to $[I_0]$. Thus, one has

$$[I_0] = [I]_0 e^{-k_d t} \quad \text{and} \quad m_0 = [I]_0(1 - e^{-k_d t}) \tag{47}$$

For the moments m_1 and m_2, we derived the kinetic equations[16]

$$\frac{dm_1}{dt} = -\frac{d[M]}{dt} \tag{48}$$

$$\frac{dm_2}{dt} = -\frac{d[M]}{dt} + 2k_p[M]m_1(R) \tag{49}$$

where $m_1(R) = \sum_{n=1}^{\infty} n[R_n]$. By integration of eq 48 and use of eq 47, one obtains the number-average degree of polymerization $X_N = m_1/m_0$ (24). To calculate m_2 and the polydispersity index PDI $= m_0 m_2/m_1^2$, one also needs $m_1(R)$. It enters the kinetic equation for the first moment of I.[16]

$$\frac{dm_1(I)}{dt} = k_c[Y]m_1(R) - k_d m_1(I) \tag{50}$$

In a controlled process most of the monomer will be incorporated into the dormant chains. This allows one to approximate $m_1(I) = m_1 = [M]_0 - [M]$. Insertion into eq 50, solving for $m_1(R)$, and use of the equilibrium relation (19) cast eq 49 into the form

$$\dot{m}_2 = -[\dot{M}] - 2[\dot{M}]([M]_0 - [M])/[I]_0 + 2k_p^2[M]^2[R]^2/k_d[I]_0 \tag{51}$$

Integration with the aid of eqs 18 and 22 yields m_2 and then the polydispersity index (25).

The phase space analysis visualizes the behavior of the radical concentrations and leads rather directly to the conditions for equilibria, but these can also be derived by other means.[15,17] It has also been applied to explore the effects of an additional radical generation[50] and of a direct or indirect decay of the dormant chains.[57] Examples are discussed below.[50]

B. Initial Excess of Persistent Species in Living Radical Polymerizations

In controlled polymerizations the time needed for radical formation by bond cleavage of the dormant chains or by the activating atom transfer must be much smaller than the total conversion time. Otherwise, one obtains a polymer with a large "living" fraction but little "control".[17] The latter situation corresponds to parameters close to point B in Figure 5 and has been observed for monomers with large propagation constants k_p. A counterstrategy is to add some persistent species before the reactions, and this has been used both in nitroxide-mediated systems[59,65,96,141−143] and in ATRP.[130] Actually, and especially in ATRP, traces of persistent species may always be present as impurities. The initial excess $[Y]_0$ first levels the transient radical concentration to the equilibrium value[130] $[R]_s = K[I]_0/[Y]_0$, and this is smaller than the radical concentration without the initial excess of the persistent species. Therefore, the conversion rate it lowered, and one obtains a linear time dependence of $\ln([M]_0/[M])$.

In a closer examination,[50] we cover only radical formation (activation) by bond cleavage and cases for which the conditions (20) for the dynamical equilibrium are fulfilled. The initial presence of the persistent species leads to the stoichiometry relations $[I]_0 - [I] = [Y] - [Y]_0 = [R] + [P]$. A comparison with the earlier relations $[I]_0 - [I] = [Y] = [R] + [P]$ suggests a new time-dependent variable, namely, the persistent radical concentration that arises only from the initiator, $[Y] - [Y]_0$. Consequently, the appropriate new reduced variable $\tilde{\eta}$ is now defined by $\tilde{\eta} = ([Y] - [Y]_0)/[I]_0$, and one has $\eta = \tilde{\eta} + \eta_0$.

The kinetic equations become

$$\dot{\rho} = 1 - \tilde{\eta} - a\rho(\tilde{\eta} + \eta_0) - b\rho^2 \tag{53}$$

$$\dot{\tilde{\eta}} = 1 - \tilde{\eta} - a\rho(\tilde{\eta} + \eta_0) \tag{54}$$

and can again be analyzed with the aid of the phase diagram. The isoclines $\tilde{\eta}_1(\rho)$, where $\dot{\tilde{\eta}} = 0$, and $\tilde{\eta}_2(\rho)$, where $\dot{\rho} = 0$, are

$$\tilde{\eta}_1(\rho) = \frac{1 - a\rho\eta_0}{1 + a\rho} \quad \text{and} \quad \tilde{\eta}_2(\rho) = \frac{1 + a\rho\eta_0 - b\rho^2}{1 + a\rho} \tag{55}$$

Figure 10 shows these isoclines in a log−log representation for different excess concentrations η_0 and for parameters fulfilling the usual equilibrium

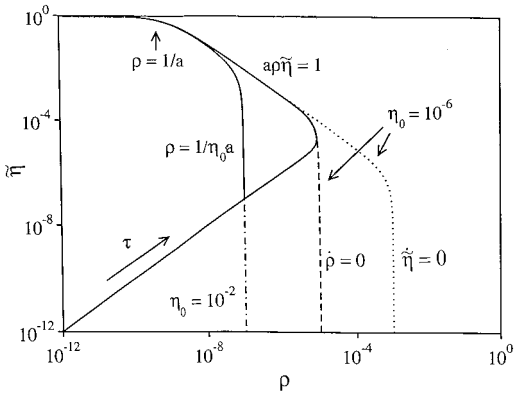

Figure 10. Trajectories of the point $(\rho,\tilde{\eta})$, that is, the reduced concentrations of the radicals $R^\bullet$ and $Y^\bullet$, and the isoclines $\dot{\rho} = 0$ (dashed) and $\dot{\tilde{\eta}} = 0$ (dotted) in the phase plane and in a log−log representation for different initial concentrations η_0 of the persistent species. Parameters $(a, b) = (10^9, 10^{10})$.

condition $a^2/b \gg 1$. The isoclines intersect the ρ-axis at

$$\rho_1 = 1/a\eta_0 \quad \text{and}$$

$$\rho_2 = (a\eta_0/2b)(\sqrt{1 + 4b/(a\eta_0)^2} - 1) \quad (56)$$

and these intersections nearly coincide if $\eta_0 \gg \sqrt{b}/a$. For the present parameters this holds for $\eta_0 \gg 10^{-4}$, and is fulfilled for $\eta_0 = 10^{-2}$, as seen in Figure 10. The isoclines are also again superimposed in a region where they satisfy the equilibrium relation $a\tilde{\eta}\rho = 1$.

Figure 10 also displays trajectories. As before, they start along the first diagonal, cross isocline $\tilde{\eta}_2$, and remain confined to the region between $\tilde{\eta}_2$ and $\tilde{\eta}_1$, thereafter. For the small $\eta_0 = 10^{-6}$, the first stage of the time evolution is directly followed by the equilibrium regime $a\tilde{\eta}\rho = 1$, that is, the trajectory is not at all influenced by the initial presence of the persistent species. For $\eta_0 = 10^{-2}$, there is an intermediate region where ρ is constant. Here, one has $a\eta_0\rho = 1$, and $a\tilde{\eta}\rho = 1$ is reached only later. In this case, and more generally for $\eta_0 \gg \sqrt{b}/a$, the two regimes can be combined to $a(\tilde{\eta} + \eta_0)\rho = 1$, that is, the usual equilibrium relation 19.

It is important to notice that for a sufficiently large excess of the persistent species $\eta_0 \gg \sqrt{b}/a$, the intermediate region where ρ is constant and one has $a\eta_0\rho = 1$ does exist even if the dynamic equilibrium 19 does not hold in the absence of the excess $[Y]_0$. Hence, in such unfavorable cases, one can drive the system to equilibrium by a deliberate addition of the persistent radical and, consequently, to control.

Figure 11 shows the radical concentrations [R] and $[Y] - [Y]_0$ versus time in a log−log representation for the same parameters a and b as used for Figure 10 and, specifically, for $k_d = 10^{-3}$ s^{-1}, $k_c = 10^7$ M^{-1} s^{-1}, $k_t = 10^8$ M^{-1} s^{-1}, and $[I]_0 = 0.1$ M. A too small initial excess $[Y]_0 = 10^{-7}$ M has no effect on the time evolution (compare Figure 1 for $k_{tY} = 0$). For the larger $[Y]_0 = 10^{-3}$ M, the short time increase of $[Y] - [Y]_0$ and [R] (Figure 10) is followed by a regime where [R] is constant at $[R] = K[I]_0/[Y]_0$. This corresponds to the vertical part of the trajectory in Figure 10. It is entered at the time $t_0 = 1/k_c[Y]_0$, where [R] obeys $[R] = k_d[I]_0t_0 = K[I]_0/[Y]_0$, and this is in the millisecond region. After the long time $t_1 = [Y]_0 3/3K^2[I]_0^2k_t$, eqs 19 hold, then [R] decreases proportionally to $t^{-1/3}$. While [R] is constant, $[Y] - [Y]_0$ takes the same value as [R] at first, then it increases linearly with time. Finally, for $t \gg t_1$, $[Y] - [Y]_0$ increases proportionally to $t^{1/3}$.

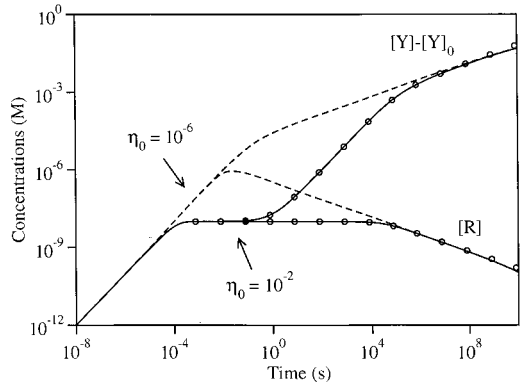

Figure 11. Time dependence of the reduced radical concentrations in a log−log representation for different reduced excess concentrations η_0 of the persistent species. Parameters a and b as used for Figure 10, and specifically $k_d = 10^{-3}$ s^{-1}, $k_c = 10^7$ M^{-1} s^{-1}, $k_t = 10^8$ M^{-1} s^{-1}, and $[I]_0 = 0.1$ M. Circles are added according to the analytical equations.

Analytical solutions that cover both the intermediate and the final time regimes are also available. Equation 44 is independent of the initial conditions and can be integrated using the combined equilibrium relation $a(\tilde{\eta} + \eta_0)\rho = 1$. As for $\eta_0 = 0$,[16] this yields an implicit equation for the time dependence of η, which leads to the approximate solution

$$[Y] = (3k_tK^2[I]_0^2(t - t_0) + [Y]_0^3)^{1/3} + K[I]_0/[Y]_0 \quad (57)$$

Apart from the small last term, it has been given earlier by Fukuda et al.[49]

With [R] given by $[R]_s = K[I]_0/[Y]_0$ before the time t_1 and by eq 18 thereafter, the rate equation for the monomer consumption (21) integrates to

$$\ln\frac{[M]_0}{[M]} = k_pK\frac{[I]_0}{[Y]_0}t \quad \text{for } t < t_1 \quad (58a)$$

and to

$$\ln\frac{[M]_0}{[M]} = k_pK\frac{[I]_0}{[Y]_0}t_1 + \frac{3}{2}k_p\left(\frac{K[I]_0}{3k_t}\right)^{1/3}(t^{2/3} - t_1^{2/3}) \quad \text{for } t > t_1 \quad (58b)$$

These relations reveal that the additional persistent species has no influence on the conversion rate if $[Y]_0 < (3K[I]_0k_t/k_p)^{1/2}$, whereas 90% conversion occurs before t_1 if $[Y]_0 > (3\ln(10)K[I]_0k_t/k_p)^{1/2}$. For a monomer with a large propagation constant of $k_p = 20\,000$ M^{-1} s^{-1}, and $k_d = 10^{-3}$ s^{-1}, $k_c = 10^7$ M^{-1} s^{-1}, $k_t = 10^8$ M^{-1} s^{-1}, and $[I]_0 = 0.1$ M, the first condition holds for $[Y]_0/[I]_0 < 0.004$, that is, 0.4% initial persistent species, and the second for $[Y]_0/[I]_0 > 0.006$, or 0.6%. Since one often applies persistent radical concentrations that are a few percent of the initiator concentration,[59,65,96,130,141−143] the second situation is met in practice. Then, eq 58a holds, that is, the polymerization index increases linearly with time and depends on the equilibrium constant. Of course, the conversion is retarded. From the previous equations one obtains the ratio between the times for 90% monomer conversion and the ratio of the unreactive products with and without the initial excess of the persistent species as

$$\frac{t_{90}([Y]_0)}{t_{90}([Y]_0 = 0)} = \frac{3}{2}[Y]_0(k_p/2\ln(10)K[I]_0k_t)^{1/2} = \frac{3}{4}\frac{[P]_{90}([Y]_0 = 0)}{[P]_{90}([Y]_0)} \quad (59)$$

For the parameters used above, this yields an about 50-fold reduction of the unreactive products for 1% excess of the persistent species at the expense of an

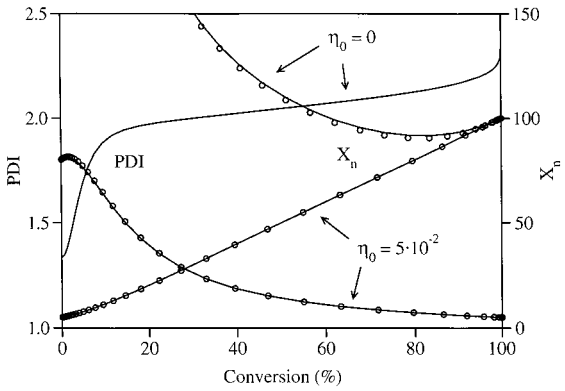

Figure 12. Average degrees of polymerization X_N and polydispersity indices as functions of conversion for a fast propagating monomer in the absence and in the presence of an initial reduced excess concentration η_0 of the persistent species. Parameters as used for Figure 11, and k_p = 20000 M^{-1} s^{-1}, $[M]_0$ = 10 M. Circles are added according to the analytical equations.

increase of the conversion time by a factor of 30. In ATRP systems, the effects are less drastic.[66]

In the derivation of the moments one has now to consider the reformation of the initiator I_0 by coupling of R_0 with the excess $Y^\bullet$, which competes with the addition of $R_0^\bullet$ to the monomer. This leads to a reduction of the effective decay rate constant of I_0 by the probability factor $\beta = k_p[M]_0/(k_p[M]_0 + k_c[Y]_0)$, so that the zeroth moment is now given by $m_0 = [I]_0(1 - e^{-\beta k_d t})$. The other equations for the moments are not changed by the presence of $[Y]_0$. Therefore, X_N is given by eq 24 with k_d replaced by βk_d.

In most cases, the excess $[Y]_0$ leads to a constant radical concentration $[R]_s = K[I]_0/[Y]_0$ during the polymerization. Insertion into eq 51, integration, and use of the definition provide the polydispersity index

$$\mathrm{PDI} = (1 - e^{-\beta k_d t})\left(1 + \frac{k_p[I]_0}{k_c[Y]_0}\frac{2 - C}{C}\right) + \frac{1}{X_N} \quad (60)$$

For small conversions but sufficiently long times, this reduces to eq 38.

Figure 12 shows the beneficial effects of 5% excess persistent species on the control of the chain length distribution for a rather fast living polymerization that shows little control without the excess, because the parameters are close to point B in Figure 5. Of course, the much better control is obtained at the expense of a strong retardation of the monomer conversion that amounts to a factor of 150. For fast polymerizations and parameters close to point C in Figure 5, one expects control but little livingness for large conversions, and in this case the improvement requires quite large initial nitroxide concentrations.[50]

C. Decay or Removal of Persistent Species in Living Radical Polymerizations

A strategy to shorten conversion times in slow living radical polymerizations is the reduction of the retarding growth of the persistent radical concentration by their removal through additives or a built-in instability.[31,118] It is likely that both procedures involve the conversion of the persistent species to a transient radical that starts a new chain. Hence, the rate increase will cause some loss of control. Here, we explore the effect of the conversion by a first-order process[50]

$$Y^\bullet \rightarrow X + R^\bullet \quad (61)$$

with rate constant k_Y.

Initially, only the initiator I shall be present. This leads to the stoichiometry relations $[I]_0 - [I] = [Y] + [X] = [R] + [P] - [X]$. Obviously, one needs to consider now three time-dependent variables, and the rate equations are

$$d[R]/dt = k_d([I]_0 - [Y] - [X]) - k_c[R][Y] + k_Y[Y] - k_t[R]^2$$

$$d[Y]/dt = k_d([I]_0 - [Y] - [X]) - k_Y[Y] - k_c[R][Y]$$

$$d[X]/dt = k_Y[Y]$$

Using the reduced variables (41) and, in addition, $\xi = [X]/[I]_0$ and $d = k_Y/k_d$ yields

$$\dot{\rho} = 1 - \eta - \xi - a\rho\eta + d\eta - b\rho^2 \quad (62a)$$

$$\dot{\eta} = 1 - \eta - \xi - a\rho\eta - d\eta \quad (62b)$$

$$\dot{\xi} = d\eta \quad (62c)$$

In the three-dimensional phase space (ρ,η,ξ) the isoclines $\eta_1(\rho)$ and $\eta_2(\rho)$ are now surfaces that intersect at

$$2d\eta = b\rho^2 \quad (63)$$

Figure 13 displays these isoclines for $\xi = 0$ and for the parameters $k_d = k_Y = 3 \times 10^{-3}$ s^{-1}, $k_c = 5\cdot10^7$ M^{-1} s^{-1}, $k_t = 10^8$ M^{-1} s^{-1}, and $[I]_0 = 0.1$ M, which obey the conditions 20. It also shows the projection of a trajectory onto the plane $(\rho,\eta,0)$. As before, after crossing η_2, the trajectory is confined to the space between the isoclines. At first, it behaves like the trajectory in Figure 9. ξ is very small in this regime and can be obtained by integrating eq 62c with η

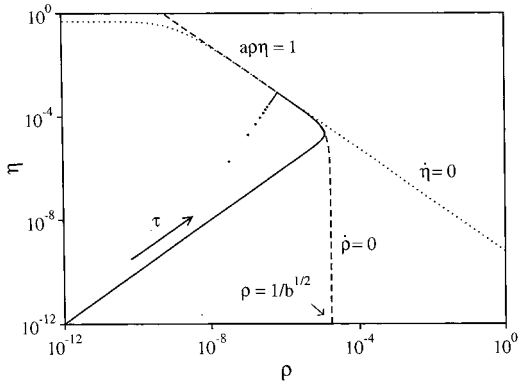

Figure 13. The isoclines $\dot{\rho} = 0$ (dashed) and $\dot{\eta} = 0$ (dotted) in the phase plane $(\rho,\eta,0)$ and a log−log representation, and the trajectory of the point (ρ,η,ξ), that is, the reduced concentrations of the radicals $R^\bullet$ and $Y^\bullet$ and the fragment X, projected onto the plane $(\rho,\eta,0)$. Parameters: $k_d = k_Y = 3 \times 10^{-3}$ s^{-1}, $k_c = 5 \times 10^7$ M^{-1} s^{-1}, $k_t = 10^8$ M^{-1} s^{-1}, and $[I]_0 = 0.1$ M.

given by eq 18. Then, the trajectory reaches the intersection (63), and the equilibrium equation changes to

$$a\rho\eta = 1 - \xi \tag{64}$$

In this regime, eqs 63 and 64 can be combined to express η by ξ only, and integration of eq 62c yields, with the proper resubstitutions,

$$[X] = [I]_0(1 + (t/t_1 - 1)^3)$$

$t_1 = 3(2[I]_0/K^2k_tk_Y^2)^{1/3}$ is the time where [X] becomes equal to $[I]_0$ and the reactions stop. Knowing [X], one finds the radical concentrations

$$[R] = \left(\frac{2k_YK[I]_0}{k_t}\right)^{1/3}(1 - t/t_1) \quad \text{and}$$

$$[Y] = \left(\frac{K^2[I]_0^2k_t}{k_Y}\right)^{1/3}(1 - t/t_1)^2 \tag{65}$$

Figure 14 shows the concentrations of all species in a log−log-representation as functions of time for the parameters given above. As qualitatively expected, the decay of Y$^\bullet$ leads to an intermediate stationary state of the radical concentrations. This state is entered at the time $t_0 = 1/6k_Y$, and for $k_Y = 3 \times 10^{-3}$ s^{-1}, this is at $t_0 = 56$ s. It breaks down at the much larger time $t_1 \approx 1.2 \times 10^7$ s = 3300 h. This may seem surprising, because the natural lifetime of Y$^\bullet$ is only $1/k_Y = 330$ s. The explanation is that the unstable persistent species is present in this form only for a small fraction of time and stays essentially incorporated in the dormant chains where it does not decay. This time fraction is approximately equal to $[Y]/[I]_0 = 0.1\%$ for the region where [Y] is constant (Figure 14).

Figure 15 displays the average degrees of polymerization and polydispersities expected without and with the decay of the persistent radical and for the parameters given above. The control remains satisfactory, even for the large decay constant k_Y. On the other hand, the time for 90% conversion is reduced by a factor of about 6. The fraction of unreactive products increases by a factor of 5 but remains small (4%). This confirms the strategy to shorten conversion times in slow living radical polymerizations by the removal of these species through additives or a built-in instability.[31,118]

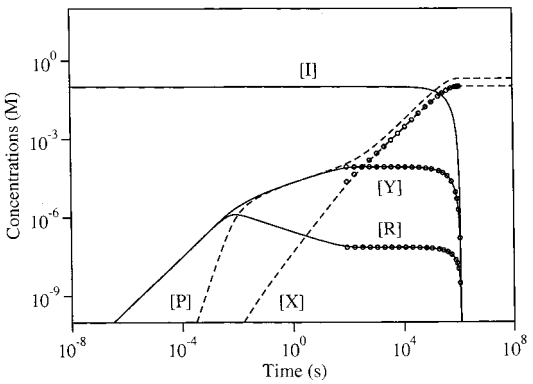

Figure 14. Radical and product concentrations versus time in a log−log representation in the absence and in the presence of a decay of the persistent species. Parameters as used for Figure 13.

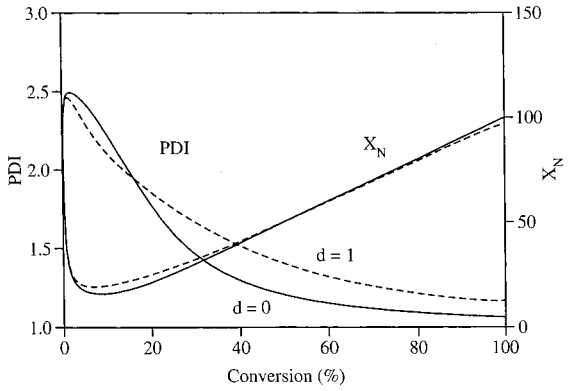

Figure 15. Average degrees of polymerization X_N and polydispersity indices as functions of conversion in the absence and in the presence of a decay of the persistent species. Parameters as used for Figure 11, and $k_p = 5000$ M^{-1} s^{-1}, $[M]_0 = 10$ M.

D. Instantaneous Radical Formation

In all examples discussed so far, the transient and the persistent species were continuously generated. Now, we consider the behavior when both radicals are initially present and then react without further generation by the cross-reaction of R$^\bullet$ with Y$^\bullet$ and by the self-terminations. This initial situation may be created by a pulse photolysis of suitable precursor molecules. The first theoretical treatment was given by O'Shaughnessy et al.,[144] and the resulting equations were later used to determine cross-reaction constants in the photocatalysis reaction of polyoxotungstates (Scheme 29).[94]

In the simplest case, the self-termination of the persistent species is absent, and the rate equations are

$$d[R]/dt = -k_c[R][Y] - k_t[R]^2 \tag{66}$$

$$d[Y]/dt = -k_c[R][Y] \tag{67}$$

with the initial concentrations $[R]_0$ and $[Y]_0$. According to eq 66, the transient species always reach $[R]_\infty = 0$ at infinite time. Insertion into eq 67 does not provide a value for $[Y]_\infty$. However, one can guess that the self-termination of R$^\bullet$ may lead to leftover Y$^\bullet$ and that this will depend on the initial concentrations and the rate constants.

To solve the problem, one combines eqs 66 and 67 to

$$\frac{d[R]}{d[Y]} = 1 + \frac{k_t}{k_c}\frac{[R]}{[Y]} \tag{68}$$

and introduces the auxiliary variable $[Z] = [R]/[Y]$. Differentiation of [Z] with respect to [Y] leads to an equation that is easily integrated. Use of the abbreviations $\rho = [R]/[R]_0$, $\eta = [Y]/[Y]_0$, $\alpha = k_t/k_c$, and $r = [R]_0/[Y]_0$ yields

$$\rho = (r(\alpha - 1))^{-1}\{(1 + r(\alpha - 1))\eta^{\alpha-1} - 1\}\cdot\eta \tag{69}$$

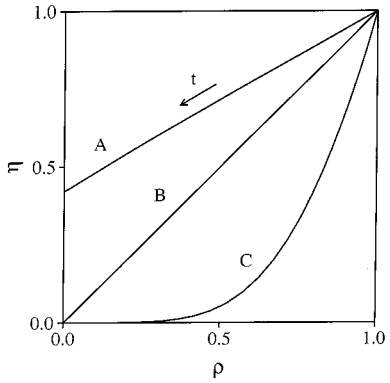

Figure 16. Trajectories of the reduced radical concentrations $\rho = [R]/[R]_0$ and $\eta = [Y]/[Y]_0$ in the phase plane for pulsed radical formation and the parameters $k_c = 5 \times 10^8$ M^{-1} s^{-1}, $k_t = 0.5k_c$ ($\alpha = 0.5$) and (A) $r^{-1} = 2(1 - \alpha)$, (B) $r^{-1} = a - 1$, and (C) $r^{-1} = (1 - \alpha)/10$.

For infinite time, where $\rho = 0$, eq 69 provides two solutions for η_∞. The first is

$$\eta_\infty = \frac{1}{(1 + r(\alpha - 1))^{1/(\alpha-1)}} \qquad (70a)$$

and it is valid for $\alpha \geq 1$, that is, $k_t \geq k_c$ for all values of $r = [R]_0/[Y]_0$. For $k_t \leq k_c$, it holds if $r^{-1} = [Y]_0/[R]_0 \geq 1 - k_t/k_c$. The second solution is

$$\eta_\infty = 0 \qquad (70b)$$

and this is obeyed for $k_t \leq k_c$ if $r^{-1} = [Y]_0/[R]_0 < 1 - k_t/k_c$. Hence, for rate constants leading to the solution (65a), one obtains the surprising result of leftover Y$^\bullet$, even if very little of this species is produced.[144] In the special case $k_t = k_c$, the final fraction of Y$^\bullet$ is $\eta_\infty = e^{-[R]_0/[Y]_0}$. Moreover, one can show that the curvature of $\eta(\rho)$, that is, of the trajectory in phase space, is negative when eq 70a is reached and positive when there is no leftover. Figure 16 provides an example for the time dependencies of the reduced concentrations.

Equation 70a has been used to extract the ratio of rate constants from the final fraction of Y$^\bullet$ in the reactions of Scheme 29.[94] The cross-reaction rate constant was found to be considerably smaller than diffusion-controlled values, and it is similar to the rate constants for the coupling of transient radicals with nitroxides (Table 1) or the deactivation step in ATRP (Table 2).

O'Shaughnessy et al.[144] have also considered a slow self-termination of the persistent radicals. The results are similar to those given above, except for a slow decay of Y$^\bullet$, which sets in when the concentration given by eq 70a is approximately reached. The authors termed the phenomenon of leftover Y$^\bullet$ a kinetic isolation of persistent radicals and suggested applications in diverse polymer−polymer reactions.

V. Concluding Remarks

Whenever in a chemical system transient and persistent radicals are formed with equal or similar rates, be it from the same or different precursors, their cross-reaction products are produced with a surprisingly high selectivity, and the otherwise prominent self-termination products of the transient radicals are virtually absent. This is not because the self-termination reaction does not take place at all. Quite on the contrary, this reaction combined with the reluctance of persistent species to undergo any self-termination causes a buildup of a considerable excess of the persistent over the transient species, and this excess then steers the reaction system toward the cross-reaction channel. Hence, the system orders itself in time, and the self-termination reaction of the transient radicals is important but it causes its own suppression.[12]

This is the basic principle of the persistent radical effect. As shown in this review, there are many variants, because there are additional reversible and irreversible reactions of the transient radicals, but these do not alter the essentials. Although it is quite natural, the principle seems somehow paradoxical, and it is not easily accepted on first sight. It took a long time from its first formulation in 1936[5] and several reinventions[6,12] until it is now clearly recognized that it operates in rather diverse branches of chemistry. This review is a first attempt to cover all major aspects and to illustrate them with examples from different fields.

Quite obviously, the often surprisingly high selectivity of the cross-reaction product formation must appeal to synthetic chemists. Whereas most of the examples known today were found accidentally without prior knowledge of the underlying principle, useful and directed new syntheses based on a better understanding are now emerging.[4,81] Since there are many types of persistent radicals and other intermediates that can take their role, one may envisage a multitude of new developments.

In polymer chemistry, the persistent radical effect can provide living and controlled radical polymerizations as a way to create new materials with very promising properties. First products seem to appear at the horizon. Here again, several rediscoveries were needed until the basics became clear.[19,29,35] At present, the fundamental and applied research is so active that it becomes difficult to follow, but fortunately, this field is also covered in two other reviews of this issue.

The nonlinear and coupled kinetic equations associated with the phenomenon lead to very surprising and not easily foreseeable rate laws. Their derivation requires mathematical tools that go beyond the usual methods of reaction kinetics, and we expect that the further exploration of reaction variants will reveal additional fascinating kinetic aspects.

Finally, in the past decades of radical chemistry the once active research on the possible types, properties, and structures of persistent radicals and related species was considered boring and unrewarding. Undoubtedly, the new possibilities offered by the persistent radical effect will lead to the rejuvenation of such research.

VI. Acknowledgment

I thank my co-workers G. Ananchenko, T. Kothe, S. Marque, R. Martschke, D. Rueegge, J. Sobek, and M. Souaille for their most important contributions;

A. Studer (Marburg), T. Fukuda (Kyoto), and K. Matyjaszewski (Pittsburgh) for useful correspondence and discussions; and the Swiss National Foundation for Scientific Research for financial support.

VII. References

(1) Griller, D.; Ingold, K. U. *Acc. Chem. Res.* **1976**, *9*, 13. In the context of this review, radicals are called persistent if their lifetimes in liquid solution exceed those of reactive radical species by many orders of magnitude. They may self-terminate slowly or disappear by other reactions, but these processes do not compete with the cross-coupling with usual transient radicals. Stable radicals can be isolated in pure form. They are included in our definition of persistence.

(2) Young, R. J.; Lovell, P. A. *Introduction to Polymers*, 2nd ed.; Chapman & Hall: London, 1991. Elias, H.-G. *Macromolecules*, 2nd ed.; Plenum: New York, 1984.

(3) Szwarc, M. *Nature* (*London*) **1956**, *198*, 1168. *J. Polym. Sci.* **1998**, *A 36*, ix.

(4) The operation of the Persistent Radical Effect in organic chemistry has lucidly been described: Studer, A. *Chem. Eur. J.* **2000**, *7*, 1159.

(5) Bachmann, W. E.; Wiselogle, F. Y. *J. Org. Chem.* **1936**, *1*, 354.

(6) Perkins, M. J. *J. Chem. Soc.* **1964**, 5932.

(7) Hey, D. H.; Perkins, M. J.; Williams, *Tetrahedron Lett.* **1963**, 445.

(8) Russell, G. A.; Bridger, R. F. *Tetrahedron Lett.* **1963**, 737. Bridger, R. F.; Russell, G. A. *J. Am. Chem. Soc.* **1963**, *85*, 3754. Huisgen, R.; Nakaten, H. *Annalen* **1954**, *586*, 70. See also: Grashey, R.; Huisgen. R. *Chem. Ber.* **1959**, *92*, 2641.

(9) Perkins, M. J. In *Free Radicals*; Kochi, J. K., Ed., Wiley: New York, 1973; Vol II, p 231 ff. Perkins, M. J. *Radical Chemistry*; Ellis Horwood, London, 1985.

(10) Geiger, G.; Huber, J. R. *Helv. Chim. Acta* **1981**, *64*, 0989, and private communication.

(11) Kraeutler, B. *Helv. Chim. Acta* **1984**, *67*, 1053.

(12) Fischer, H, *J. Am. Chem. Soc.* **1986**, *108*, 3925.

(13) To avoid the crowding of subsequent formulae by factors of 2, we define the self-termination rates here by, for example, $d[R]/dt = -k_{tR}[R]^2$, deviating from the IUPAC convention.

(14) An explanation of excess cross-coupling products by different rate constants for the homocoupling reactions has also been given: P. J. Wagner. Wagner, P. J.; Thomas, M. J.; Puchalski, A. E. *J. Am. Chem. Soc.* **1986**, *108*, 7739.

(15) Fischer, H. *Macromolecules* **1997**, *30*, 5666.

(16) Fischer, H. *J. Polymer Sci., Part A: Polym. Chem.* **1999**, *37*, 1885.

(17) Souaille, M.; Fischer, H. *Macromolecules* **2000**, *33*, 7378.

(18) Depending on the ratio k_c/k_{tR}, other solutions hold in the transition period between the initial linear increase and the behavior given by eqs 8.[17]

(19) An easy derivation of the third root dependence of the radical concentrations with preassumption of the equilibrium was first presented by Fukuda et al.: Ohno, K.; Tsujii, Y.; Miyamozo, T.; Fukuda, T.; Goto, A.; Kobayashi, K.; Akaike, T. *Macromolecules* **1998**, *31*, 1064. These authors also gave an early and clear description of the basic reaction principles: Fukuda, T.; Terauchi, T.; Goto, A.; Ohno, K.; Tsujii, Y.; Miyamoto, T.; Kobatake, S.; Yamada, B. *Macromolecules* **1996**, *29*, 6393.

(20) Rueegge, D.; Fischer, H. *Int. J. Chem. Kinet.* **1989**, *21*, 703.

(21) Daikh, B. E.; Finke, R. G. *J. Am. Chem. Soc.* **1992**, *114*, 2938.

(22) Kothe, T.; Marque, S.; Martschke, R.; Popov, M.; Fischer, H. *J. Chem. Soc. Perkin* Trans. *2*, **1998**, 1553.

(23) Kothe, T. Ph.D. Thesis, Zuerich, **2001**.

(24) Otsu, T.; Yoshida, M. *Makromol. Chem. Rapid Commun.* **1982**, *3*, 127. Otsu, T.; Yoshida, M. *Makromol. Chem. Rapid Commun.* **1982**, *3*, 133. Otsu, T.; Matsunaga, T.; Kuriyama, A.; Yoshioka, M. *Eur. Polym. J.* **1989**, *25*, 643, and references therein. In a lucid highlight, Prof. Otsu has recently reviewed his work and the iniferter technique. An iniferter is a compound the fragments of which *ini*tiate and preferably cross-*ter*minate by primary radical termination and which is subject to chain trans*fer* from the propagating species, although for many of Otsu's examples chain transfer is unlikely. Otsu, T. *J. Polym. Sci., Part A: Polym. Chem.* **2000**, *38*, 2121.

(25) Bledzki, A.; Braun, D. *Makromol. Chem.* **1981**, *182*, 1047. Braun, D. Skrzek, T.; Steinhauer-Beisser, S. Tretner, H.; Lindner, H. J. *Macromol. Chem. Phys.* **1995**, *196*, 573, and references therein.

(26) Otsu, T.; Tazaki, T.; Yoshioka, M. *Chem. Express* **1990**, *5*, 801.

(27) Solomon, D. H., Rizzardo, E.; Cacioli, P. U.S. Patent 4581429, March 27, 1985.

(28) Rizzardo, E. *Chem. Aust.* **1987**, *54*, 32.

(29) Johnson, C. H.; Moad, G.; Solomon, D. H.; Spurling, T. H.; Vearing, D. J. *Aust. J. Chem.* **1990**, *43*, 1215.

(30) Georges, M. K.; Veregin, R. P. N.; Kazmaier, P. M.; Hamer, G. K. *Macromolecules* **1993**, *26*, 2987.

(31) Georges, M. K.; Veregin, R. P. N.; Kazmaier, P. M.; Hamer, G. K.; Saban, M. D. *Macromolecules* **1994**, *27*, 7228. Saban, M. D.; Georges, M. K.; Veregin, R. P. N.; Hamer, G. K.; Kazmaier, P. M. *Macromolecules* **1995**, *28*, 7032. Veregin, R. P. N.; Odell, P. G.; Michalak, L. M.; Georges, M. K. *Macromolecules* **1996**, *29*, 2746. Georges, M. K.; Hamer, G. K.; Listigovers, N. A. *Macromolecules* **1998**, *31*, 9087. MacLeod, P. J.; Veregin, R. P. N.; Odell, P. G.; Georges, M. K. *Macromolecules* **1998**, *31*, 530. Moffat, K. A.; Hamer, G. K.; Georges, M. K. *Macromolecules* **1999**, *32*, 1004, and references therein.

(32) Hawker, C. J.; Barclay, G. G.; Dao, J. *J. Am. Chem. Soc.* **1996**, *118*, 11467.

(33) (a) Li, I.; Howell, B. A.; Matyjaszewski, K.; Shigemoto, T.; Smith, P. B.; Priddy, D. B. *Macromolecules* **1995**, *28*, 6692. (b) Hawker, C. J.; Barclay, G. G.; Orellana, A.; Dao, J.; Devonport, W. *Macromolecules* **1996**, *29*, 5245.

(34) Catala, J. M.; Bubel, F.; Oulad Hammouch, S. *Macromolecules* **1995**, *28*, 8441. Oulad Hammouch, S.; Catala, J. M. *Macromol. Rapid Commun.* **1996**, *17*, 8841.

(35) (a) Greszta, D.; Matyjaszewski, K. *Macromolecules* **1996**, *29*, 5239. (b) Greszta, D.; Matyjaszewski, K. *Macromolecules* **1996**, *29*, 7661.

(36) (a) Greszta, D.; Matyjaszewski, K. *J. Polym. Sci., Part A: Polym. Chem.* **1997**, *35*, 1857. (b) Goto, A.; Fukuda, T. *Macromolecules* **1997**, *30*, 4272.

(37) Wayland, B. B.; Pozmik, G.; Mukerjee, S. L. *J. Am. Chem. Soc.* **1994**, *116*, 7943.

(38) Suess, H.; Pilch, K.; Rudorfer, H. *Z. Phys. Chem.* **1937**, *A179*, 361. Mayo, F. R. *J. Am. Chem. Soc.* **1943**, *65*, 2324. Kharasch, M. S.; Jensen, E. V.; Urry, W. H. *Science* **1945**, *102*, 128.

(39) Minisci, F.; Pallini, U. *Gazz. Chim. Ital.* **1961**, *91*, 1030. Minisci, F. *Acc. Chem. Res.* **1975**, *8*, 165.

(40) Asscher, M.; Vofsi, D. *J. Chem. Soc.* **1961**, 22611. Asscher, M.; Vofsi, D. *J. Chem. Soc.* **1963**, *1887*, 3921.

(41) (a) Julia, M.; Le Thuillier, G.; Saussine, L. *J. Organomet. Chem.* **1979**, *177*, 128. (b) Matsumoto, H.; Nakano, T.; Nagai, Y. *Tetrahedron Lett.* **1973**, *51*, 5147.

(42) Kato, M., Kamigato, M.; Sawamoto, M.; Higashimura, T. *Macromolecules* **1995**, *28*, 1721.

(43) Wang, J.-S.; Matyjaszewski, K. *J. Am. Chem. Soc.* **1995**, *117*, 5614.

(44) Percec, V.; Barboiu, B. *Macromolecules* **1995**, *28*, 7970.

(45) Darling, T. R.; Davis, T. P.; Fryd, M.; Gridnev, A. A.; Haddleton, D. M.; Ittel, S. D.; Matheson, R. R. Jr.; Moad, G.; Rizzardo, E. *J. Polym. Sci., Part A: Polym. Chem.* **2000**, *38*, 1709, and the following comments.

(46) Shipp, D. A.; Matyjaszewski, K. *Macromolecules* **1999**, *32*, 2948.

(47) He, J.; Zhang, H.; Chen, J.; Yang, Y. *Macromolecules* **1997**, *30*, 8010. He, J.; Li, L.; Yang, Y. *Macromolecules* **2000**, *33*, 2286. He, J.; Chen, J.; Li, L.; Pan, J.; Li, C.; Cao, J.; Tao, Y.; Hua, F.; Yang, Y.; McKee, G. E.; Brinkmann, S. *Polymer* **2000**, *41*, 4573, and references therein.

(48) Fukuda, T.; Goto, A.; Ohno, K. *Macromol. Rapid Commun.* **2000**, *21*, 151.

(49) Fukuda, T.; Goto, A. *ACS Symp. Ser.* **2000**, *768*, 27. Goto, A.; Fukuda, T. *Macromol. Chem. Phys.* **2000**, *201*, 2138, and references therein.

(50) Souaille, M.; Fischer, H. *Macromolecules* **2001**, in press.

(51) Moad, G.; Anderson, A. G.; Ercole, F.; Johnson, C. H. J.; Krstina, J.; Moad, C. L.; Rizzardo, E.; Spurling, T. H.; Thang, S. H. *ACS Symp. Ser.* **1998**, *685*, 332.

(52) Skene, W. G.; Scaiano, J. C.; Listigovers, N. A.; Kazmaier, P. M.; Georges, M. K. *Macromolecules* **2000**, *33*, 5065.

(53) Tsujii, T.; Fukuda, T.; Miyamoto, T. *Polymer Preprints* **1997**, *38*, 657. Ohno, K.; Tsujii, Y.; Fukuda, T. *Macromolecules* **1997**, *30*, 2503.

(54) Goto, A.; Terauchi, T.; Fukuda, T.; Miyamoto, T. *Macromol. Rapid Commun.* **1997**, *18*, 673.

(55) Goto, A.; Fukuda, T. *Macromolecules* **1999**, *32*, 618.

(56) Fukuda, T.; Goto, A. *Macromol. Rapid Commun.* **1997**, *18*, 683.

(57) Souaille, M.; Fischer, H. *Macromolecules* **2001**, *34*, 2830.

(58) Matyjaszewski, K.; Kajiwara, A. *Macromolecules* **1998**, *31*, 548. Kajiwara, A.; Matyjaszewski, K.; Kamachi, M. *ACS Symp. Ser.* **2000**, *768*, 68, and references therein.

(59) Benoit, D.; Grimaldi, S.; Robin, S.; Finet, J.-P.; Tordo, P.; Gnanou, Y. *J. Am. Chem. Soc.* **2000**, *122*, 5929.

(60) Le Mercier, C.; Lutz, J.-F.; Marque, S.; Le Moigne, F.; Tordo, P., Lacroix-Desmazes, P. Boutevin, B.; Couturier, J.-L.; Guerret, O.; Martschke, R.; Sobek, J.; Fischer, H. *ACS Symp. Ser.* **2000**, *768*, 108, and references therein.

(61) Lutz, J. F.; Lacroix-Desmazes, P.; Boutevin, B. *Macromol. Chem. Phys.* **2000**, *201*, 662.

(62) Marque, S.; LeMercier, C.; Tordo, P.; Fischer, H. *Macromolecules* **2000**, *33*, 4403.

(63) Sobek, J.; Martschke, R.; Fischer, H. *J. Am. Chem. Soc.* **2001**, *123*, 2849, and references therein.

(64) Ohno, K.; Goto, A.; Fukuda, T.; Xia, J.; Matyjaszewski, K. *Macromolecules* **1998**, *31*, 2699.
(65) Lutz, J.-F.; Lacroix-Desmazes, P.; Boutevin, B. *Macromol. Rapid Commun.* **2001**, *22*, 189.
(66) Chambard, G.; Klumpermann, B. *ACS Symp. Ser.* **2000**, *768*, 197. Zhang, H.; Klumperman, B.; Ming, W.; Fischer, H.; van der Linde, R. *Macromolecules*, **2001**, submitted.
(67) Chiefari, J.; Chong, Y. K.; Ercole, F.; Krstina, J.; Jeffery, J.; Lee, T. P. T.; Mayadunne, R. T. A.; Meijs, G. F.; Moad, C. L.; Moad, G.; Rizzardo, E.; Thang, S. H. *Macromolecules* **1998**, *31*, 5559.
(68) Matyjaszewski, K.; Gaynor, S.; Wang, J.-S. *Macromolecules* **1995**, *28*, 2093.
(69) Barton, D. H. R.; Beaton, J. M.; Geller, L. E.; Pechet, M. M. *J. Am. Chem. Soc.* **1960**, *82*, 2640. Akhtar, M. *Adv. Photochem.* **1964**, *2*, 263. Suginome, H.; Osada, A. *J. Chem. Soc. Perkin Trans. 1* **1982**, 1963, and references therein.
(70) Chow, Y. L. *Acc. Chem. Res.* **1973**, *6*, 354. Flesia, E.; Croatto, A.; Tordo, P.; Surzur, J.-M. *Tetrahedron Lett.* **1972**, 535, and references therein.
(71) Key references to these radicals include: Gomberg, M. *J. Am. Chem. Soc.* **1900**, *22*, 757, *Chem. Ber.* **1900**, *33*, 3150. Ballester, M.; Riera, J.; Castaner, J.; Badia, C.; Monso, J. M. *J. Am. Chem. Soc.* **1971**, *93*, 2215. Wieland, H.; Offenbaecher, H. *Chem. Ber.* **1914**, *47*, 2111. Goldschmidt, S.; Renn, K. *Chem. Ber.* **1922**, *55*, 628. Mueller, E.; Ley. K. *Z. Naturforsch. B* **1953**, *8*, 694. Ziegler, K. *Chem. Ber.* **1922**, *55*, 2257. Kosower, E. M.; Poziomek, E. J. *J. Am. Chem. Soc.* **1964**, *86*, 5515. de Vries, L. *J. Am. Chem. Soc.* **1978**, *100*, 926, and ref 1.
(72) *Landolt-Boernstein, New Series, Magnetic Properties of Free Radicals*; Hellwege, K.-H.; Fischer, H., Eds., Springer: Berlin**,** 1965−2002; Group II, Vols. 1, 9, 17, 26.
(73) *Landolt-Boernstein, New Series, Radical Reaction Rates in Liquids*; Springer: Berlin**,** 1984−1998; Group II, Vols. 13, 18.
(74) Bravo, A.; Bjorsvik, H.-R.; Fontana, F.; Liguori, L.; Minisci, F. *J. Org. Chem.* **1997**, *62*, 3849.
(75) MacFaul, P. A.; Arends, I. W. C. E.; Ingold, K.; Wayner, D. D. M. *J. Chem. Soc. Perkin Trans. 2* **1997**, 135.
(76) Lucas, M. A.; Schiesser, C. H. *J. Org. Chem.* **1996**, *61*, 5754.
(77) Lepley, A. R. In *Chemically Induced Magnetic Polarization*; Lepley, A. R.; Closs, G. L. Eds., Wiley: New York, 1973.
(78) Walling, C. *J. Am. Chem. Soc.* **1988**, *110*, 6846.
(79) Yokoi, M.; Nakano, T.; Fujita, W.; Ishiguro, K.; Sawaki, Y. *J. Am. Chem. Soc.* **1998**, *120*, 12453.
(80) (a) Müller, F.; Mattay, J. *Chem. Rev.* **1993**, *93*, 99. (b) Fukuzimi, S.; Itoh, S. *Adv. Photochem.* **1999**, *25*, 107.
(81) Studer, A. *Angew. Chem. Int. Ed.* **2000**, *39*, 1108.
(82) Marque, S.; Fischer, H.; Baier, E.; Studer, A. *J. Org. Chem.* **2001**, *66*, 1146.
(83) (a) Pattenden, G. *Chem. Soc. Rev.* **1988**, *17*, 361. (b) Branchaud, B. P.; Yu, G.-X. *Organometallics* **1993**, *12*, 4262. (c) Iqbal, J.; Bhatia, B.; Nayyar, N. K. *Chem. Rev.* **1994**, *94*, 519, and references therein.
(84) Ghosez, A.; Göbel, T.; Giese, B. *Chem. Ber.* **1988**, *121*, 1807.
(85) Halpern, J. *ACS Symp. Ser.* **1990**, *428*, 100, and references therein.
(86) Scheffold, R.; Abrecht, S.; Orlinski, R.; Ruf, H.-R.; Stamouli, P.; Tinembart, O.; Walder, L.; Weymuth, C. *Pure Appl. Chem.* **1987**, *59*, 363.
(87) House, D. A. *Adv. Inorg. Chem.* **1997**, *44*, 341, and references therein.
(88) Van Vliet, M. R. P.; Jastrzebski, J. T. B. H.; van Koten, G.; Vrieze, K.; Spek, A. L. *J. Organometal. Chem.* **1981**, *210*, C49. Wissing, E.; Jstrzebski, J. T. B. H.; Boersma, J.; van Koten, G. *J. Organometal. Chem.* **1993**, *459*, 11, and references therein.
(89) (a) Bellus, D. *Pure Appl. Chem.* **1985**, *57*, 1827. (b) Boutevin, B. *J. Polym. Sci., Part A: Polym. Chem.* **2000**, *38*, 3235.
(90) Gossage, R. A.; van de Kuil, L. A.; van Koten, G. *Acc. Chem. Res.* **1998**, *31*, 423.
(91) (a) Hayes, T. K.; Villani, R.; Weinreb, S. M. *J. Am. Chem. Soc.* **1988**, *110*, 5533. (b) Udding, J. H.; Tuijp, K. C. J. M.; van Zanden, M. N. A.; Hiemstra, H.; Speckamp, W. N. *J. Org. Chem.* **1994**, *59*, 1993.
(92) Matyjaszewski, K.; Paik, H.; Shipp, D. A.; Isobe, Y.; Okamoto, Y. *Macromolecules* **2001**, *34*, 3127. For related evidence, see: Matyjaszewski, K. *Macromolecules* **1998**, *31*, 4710.
(93) Jaines, B. S.; Hill, C. L. *J. Am. Chem. Soc.* **1995**, *117*, 4704. Yamase, Y.; Ohtaka, K. J. *Chem. Soc. Dalton Trans.* **1994**, 2599. Ermolenko, L. P.; Delaire, J. A.; Giannotti, C. *J. Chem. Soc. Perkin Trans. 2*, **1997**, 25. Mylonas, A.; Papaconstantinou, E. *J. Photochem. Photobiol.* **1996**, *94*, 77, and references therein.
(94) Kothe, T.; Martschke, R.; Fischer, H. *J. Chem. Soc. Perkin Trans. 2*, **1998**, 503.
(95) Hawker, C. *Chem. Rev.* **2001**, *101*, 3661−3688. Sawamoto, M.; Kamigaito, M.; Ando, T. *Chem. Rev.* **2001**, *101*, 3689−3746.
(96) Benoit, D.; Chaplinski, V.; Braslau, R.; Hawker, C. J. *J. Am. Chem. Soc.* **1999**, *121*, 3904.
(97) Chong, B. Y. K.; Ercole, F.; Moad, G.; Rizzardo, E.; Anderson, A. G. *Macromolecules* **1999**, *32*, 6896.
(98) Kramer, A.; Nesvadba, P. 1999, DE Patent 19909767A1, 1999.
(99) Connolly, T. J.; Baldovi, M. V.; Mohtat, N.; Scaiano, J. C. *Tetrahedron Lett.* **1996**, *37*, 4919.
(100) Braslau, R.; Burrill, L. C., II; Siano, M.; Naik, N.; Howden, R. K.; Mahal, L. K. *Macromolecules* **1997**, *30*, 6445.
(101) Matyjaszewski, K.; Woodworth, B. E.; Zhang, X.; Gaynor, S. G.; Metzner, Z. *Macromolecules* **1998**, *31*, 5955.
(102) Bergbreiter, D. E.; Walchuk, B. *Macromolecules* **1998**, *31*, 6380.
(103) Zink, M.-O.; Kramer, A.; Nesvadba, P. *Macromolecules* **2000**, *33*, 8106.
(104) Moad, G.; Rizzardo, E. *Macromolecules* **1995**, *28*, 8722.
(105) Skene, W. G.; Belt, S. T.; Connolly, T. J.; Hahn, P.; Scaiano, J. C. *Macromolecules* **1998**, *31*, 9103.
(106) Ciriano, M. V.; Korth, H. G.; van Scheppeningen, W. B.; Mulder, P. *J. Am. Chem. Soc.* **1999**, *121*, 6375.
(107) Bon, S. A. F.; Chambard, G.; German, A. L. *Macromolecules* **1999**, *32*, 8269.
(108) Beckwith, A. L. J.; Bowry, V. W.; Ingold, K. U. *J. Am. Chem. Soc.* **1992**, *114*, 4983. Bowry, V. W.; Ingold, K. U. *J. Am. Chem. Soc.* **1992**, *114*, 4992. Chateauneuf, J.; Lusztyk, J.; Ingold, K. U. *J. Org. Chem.* **1988**, *53*, 1629. Beckwith, A. L. J.; Bowry, V. W.; Moad, G. *J. Org. Chem.* **1988**, *53*, 1632.
(109) Baldovi, M. V.; Mohtat, N.; Scaiano, J. C. *Macromolecules* **1996**, *29*, 5497.
(110) Marsal, P.; Roche, M.; Tordo, P.; de Sainte Claire, P. *J. Phys. Chem. A* **1999**, *103*, 2899.
(111) Benson, S. W. *Thermochemical Kinetics*; Wiley: New York, 1968. Rüchardt, C.; Beckhaus, H.-D. *Angew. Chem.* **1980**, *92*, 417.
(112) Ananchenko, G. S.; Fischer, H. *J. Polym. Sci. Part A: Polym. Chem.* **2001**, in press. Ananchenko, G. S.; Souaille, M.; Fischer, H. *J. Polym. Sci. Part A: Polym. Chem.* In press.
(113) Skene, W. G.; Scaiano, J. C.; Yap, G. P. A. *Macromolecules* **2000**, *33*, 3536.
(114) Rodlert, M.; Harth, E.; Rees, I.; Hawker, C. J. *J. Polym. Sci., Part A: Polym. Chem.* **2000**, *38*, 4749.
(115) Harth, E.; Hawker, C. J.; Fan, W.; Waymouth, R. M. *Macromolecules* **2001**, *34*, 3856.
(116) Connolly, T. J.; Scaiano, J. C. *Tetrahedron Lett.* **1997**, *38*, 1133.
(117) Moad, G.; Rizzardo, E.; Solomon, D. H. *Polym. Bull.* **1982**, *6*, 589.
(118) Gridnev, A. A. *Macromolecules* **1997**, *30*, 7651.
(119) Chung, T. C.; Janvikul, W.; Lu, H. L. *J. Am. Chem. Soc.* **1996**, *118*, 705.
(120) Klapper, M.; Brand, T.; Steenbock, M.; Müllen, K. *ACS Symp. Ser.* **2000**, *768*, 152, and references therein.
(121) Yamada, T.; Nobuka, Y.; Miura, Y. *Polym. Bull.* **1998**, *41*, 1288.
(122) Wayland, B. B.; Basickes, L.; Mukerjee, S.; Wei, M.; Fryd, M. *Macromolecules* **1997**, *30*, 8105.
(123) Kickelbick, G.; Reinöhl, U.; Ertel, T. S.; Bertagnolli, H.; Matyjaszewski, K. *ACS Symp. Ser.* **2000**, *768*, 211. Kickelbick, G.; Reinöhl, U.; Ertel, T. S.; Weber, A.; Bertagnolli, H.; Matyjaszewski, K. *Inorg. Chem.* **2001**, *40*, 6. Pintauer, T.; Qiu, J.; Kickelbick, G.; Matyaszewski, K. *Inorg. Chem.* **2001**, *40*, 2818.
(124) Queffelec, J.; Gaynor, S. G.; Matyjaszewski, K. *Macromolecules* **2000**, *33*, 8629, and references therein.
(125) Ando, T.; Kamigaito, M.; Sawamoto, M. *Macromolecules* **1997**, *30*, 4507. Matyjaszewski, K.; Wei, M.; Xia, J.; McDermott, N. E. *Macromolecules* **1997**, *30*, 8161.
(126) Granel, C.; Dubois, P.; Jerome, R.; Teyssie, P. *Macromolecules* **1996**, *29*, 8576.
(127) Moineau, G.; Granel, C.; Dubois, P.; Jerome, R.; Teyssie, *Macromolecules* **1998**, *31*, 542.
(128) Lecomte, P.; Drapier, I.; Dubois, P.; Teyssie, P.; Jerome, R. *Macromolecules* **1997**, *30*, 7631.
(129) Percec, V.; Asandei, A. D.; Asgarzadeh, F.; Barboiu, B.; Holerca, M. N.; Grigoras, C. *J. Polym. Sci. Part A: Polym. Chem.* **2000**, *38*, 4353. Percec, V.; Barboiu, B.; Bera, T. K.; van der Sluis, M.; Grubbs, R. B.; Frechet, J. M. J. *J. Polym. Sci. Part A: Polym. Chem.* **2000**, *38*, 4776.
(130) Matyjaszwewski, K.; Patten, T. E.; Xia, J. *J. Am. Chem. Soc.* **1997**, *119*, 674.
(131) Davis, K. A.; Paik, H.; Matyjaszewski, K. *Macromolecules* **1999**, *32*, 1767.
(132) Xia, J.; Matyjaszewski, K. *Macromolecules* **1997**, *30*, 7697.
(133) Haddleton, D. M.; Perrier, S.; Bon, S. A. F. *Macromolecules* **2000**, *33*, 8246.
(134) Matyjaszewski, K.; Göbelt, B.; Paik, H.; Horwitz, C. P. *Macromolecules* **2001**, *34*, 430, and references therein.
(135) Johnson, R. M.; Ng, C.; Samson, C. C. M.; Fraser, C. L. *Macromolecules* **2000**, *33*, 8618.
(136) Shen, Y.; Zhu, S.; Zeng, F.; Pelton, R. H. *Macromol. Chem. Phys.* **2000**, *201*, 1169.
(137) Parker, J.; Jones, R. G.; Holder, S. J. *Macromolecules* **2000**, *33*, 9166.
(138) Acar, A. E.; Yagzi, M. B.; Mathias, L. J. *Macromolecules* **2000**, *33*, 7700.
(139) Matyjaszewski, K.; Davis, K.; Patten, T. E.; Wei, M. *Tetrahedron* **1997**, *45*, 15321.
(140) Shipp, D. A.; Matyjaszewski, K. *Macromolecules* **2000**, *33*, 1553.

(141) Benoit, D.; Hawker, C. J.; Huang, E. E.; Lin, Z.; Russell, T. P. *Macromolecules* **2000**, *33*, 1505. Benoit, D.; Harth, E.; Helms, B.; Vestberg, R.; Rodlert, M.; Hawker, C. J. *ACS Symp. Ser.* **2000**, *768*, 122.
(142) Lacroix-Desmazes, P.; Lutz, J.-F.; Boutevin, B. *Macromol. Chem. Phys.* **2000**, *210*, 662.
(143) Bon, A. F.; Bosveld, M.; Klumperman, B.; German, A. L. *Macromolecules* **1997**, *30*, 324.
(144) Karetekin, E.; O'Shaughnessy, B.; Turro, N. J. *Macromolecules* **1998**, *31*, 4655. *J. Chem. Phys.* **1998**, *108*, 9577.

CR990124Y